The Physics of Plasmas

T. J. M. Boyd and J. J. Sanderson

CAMBRIDGE

CAMBRIDGE more information - www.cambridge.org/9780521452908

This page intentionally left blank

The Physics of Plasmas

The Physics of Plasmas provides a comprehensive introduction to the subject suitable for adoption as a self-contained text for courses at advanced undergraduate and graduate level. The extensive coverage of basic theory is illustrated with examples drawn from fusion, space and astrophysical plasmas.

A particular strength of the book is its discussion of the various models used to describe plasma physics including particle orbit theory, fluid equations, ideal and resistive magnetohydrodynamics, wave equations and kinetic theory. The relationships between these distinct approaches are carefully explained giving the reader a firm grounding in the fundamentals, and developing this into an understanding of some of the more specialized topics. Throughout the text, there is an emphasis on the physical interpretation of plasma phenomena and exercises, designed to test the reader's understanding at a variety of levels, are provided.

Students of physics and astronomy, engineering and applied mathematics will find a clear and rigorous explanation of the fundamental properties of plasmas with minimal mathematical formality. This book will also serve as a reference source for physicists and engineers engaged in research on aspects of fusion and space plasmas.

Before retiring, T.J.M. BOYD was Professor of Physics at the University of Essex. He has taught graduate students on plasma physics courses in Europe and North America. His research interests have included atomic collision theory, computational physics and plasma physics. Professor Boyd has co-authored two previous books, *Plasma Dynamics* (1969) with J.J. Sanderson, and *Electricity* (1979) with C.A. Coulson.

JEFF SANDERSON is Professor Emeritus at the University of St Andrews. His research interests are in theoretical plasma physics and specifically plasma instabilities, collisionless shock waves and transport phenomena. Professor Sanderson has taught plasma physics for over 30 years, principally at St Andrews University, and the UKAEA Culham Summer School, but also by invitation in the USA, Europe and Pakistan. As well as co-authoring *Plasma Dynamics* (1969) he was a contributor to two Culham textbooks and co-editor with R.A. Cairns of *Laser Plasma Interactions* (1980).

The Physics of Plasmas

T.J.M. BOYD
University of Essex

J.J. SANDERSON
University of St Andrews

CAMBRIDGE
UNIVERSITY PRESS

CAMBRIDGE UNIVERSITY PRESS
Cambridge, New York, Melbourne, Madrid, Cape Town, Singapore, São Paulo

Cambridge University Press
The Edinburgh Building, Cambridge CB2 2RU, United Kingdom

Published in the United States of America by Cambridge University Press, New York

www.cambridge.org

Information on this title: www.cambridge.org/9780521452908

First published in print format 2003

ISBN-13 978-0-511-07420-2 eBook (Adobe Reader)
ISBN-10 0-511-07420-4 eBook (Adobe Reader)

ISBN-13 978-0-521-45290-8 hardback
ISBN-10 0-521-45290-2 hardback

ISBN-13 978-0-521-45912-9 paperback
ISBN-10 0-521-45912-5 paperback

Contents

Preface

The present book has its origins in our earlier book *Plasma Dynamics* published in 1969. Many who used *Plasma Dynamics* took the trouble to send us comments, corrections and criticism, much of which we intended to incorporate in a new edition. In the event our separate preoccupations so delayed this that we came to the conclusion that we should instead write another book, that might better reflect changes of emphasis in the subject since the original publication. In writing we had two aims. The first was to describe topics that have a place in any core curriculum for plasma physics, regardless of subsequent specialization and to do this in a way that, while keeping physical understanding firmly in mind, did not compromise on a proper mathematical framework for developing the subject. At the same time we felt the need to go a step beyond this and illustrate and extend this basic theory with examples drawn from topics in fusion and space plasma physics.

In developing the subject we have followed the traditional approach that in our experience works best, beginning with particle orbit theory. This combines the relative simplicity of describing the dynamics of a single charged particle, using concepts familiar from classical electrodynamics, before proceeding to a variety of magnetohydrodynamic (MHD) models. Some of the intrinsic difficulties in getting to grips with magnetohydrodynamics stem from the persistent neglect of classical fluid dynamics in most undergraduate physics curricula. To counter this we have included in Chapter 3 a brief outline of some basic concepts of fluid dynamics before characterizing the different MHD regimes. This leads on to a detailed account of ideal MHD in Chapter 4 followed by a selection of topics illustrating different aspects of resistive MHD in Chapter 5. Plasmas support a bewildering variety of waves and instabilities and the next two chapters are given over to classifying the most important of these. Chapter 6 continues the MHD theme, dealing with waves which can be described macroscopically. In contrast to normal fluids, plasmas are characterized by modes which have to be described microscopically, i.e. in terms of kinetic theory, because only particular particles in the distribution interact with the modes in question. An introduction to plasma kinetic theory is included in Chapter 7 along with a full discussion of the basic modes, the physics of which is governed largely by wave–particle interactions. The development of kinetic theory is continued in Chapter 8 but with a change of emphasis. Whereas the effect of

collisions between plasma particles is disregarded in Chapter 7, these move centre stage in Chapter 8 with an introduction to another key topic, plasma transport theory.

A thorough grounding in plasma physics is provided by a selection of topics from the first eight chapters, which make up a core syllabus irrespective of subsequent specialization. The remaining chapters develop the subject and provide a basis for more specialized courses, although arguably Chapter 9 on plasma radiation is properly part of any core syllabus. This chapter, which discusses the principal sources of plasma radiation, excepting bound–bound transitions, along with an outline of radiative transport and the scattering of radiation by laboratory plasmas, provides an introduction to a topic which underpins a number of key plasma diagnostics. Chapters 10 and 11 deal in turn and in different ways with aspects of non-linear plasma physics and with effects in inhomogeneous plasmas. Both subjects cover such a diversity of topics that we have been limited to a discussion of a number of examples, chosen to illustrate the methodology and physics involved. In Chapter 10 we mainly follow a tutorial approach, outlining a variety of important non-linear effects, whereas in Chapter 11 we describe in greater detail a few particular examples by way of demonstrating the effects of plasma inhomogeneity and physical boundaries. The book ends with a chapter on the classical theory of plasmas in which we outline the comprehensive mathematical structure underlying the various models used, highlighting how these relate to one another.

An essential part of getting to grips with any branch of physics is working through exercises at a variety of levels. Most chapters end with a selection of exercises ranging from simple quantitative applications of basic results on the one hand to others requiring numberical solution or reference to original papers.

We are indebted to many who have helped in a variety of ways during the long period it has taken to complete this work. For their several contributions, comments and criticism we thank Hugh Barr, Alan Cairns, Angela Dyson, Pat Edwin, Ignazio Fidone, Malcolm Haines, Alan Hood, Gordon Inverarity, David Montgomery, Ricardo Ondarza-Rovira, Sean Oughton, Eric Priest, Bernard Roberts, Steven Schwartz, Greg Tallents, Alexey Tatarinov and Andrew Wright. We are indebted to Dr J.M. Holt for permission to reproduce Fig. 9.16. Special thanks are due to Andrew Mackwood who prepared the figures and to Misha Sanderson who shared with Andrew the burden of producing much of the LaTeX copy. Finally, we thank Sally Thomas, our editor at CUP, for her ready help and advice in bringing the book to press.

T.J.M. Boyd, Dedham
J.J. Sanderson, St Andrews

1

Introduction

1.1 Introduction

The plasma state is often referred to as the *fourth* state of matter, an identification that resonates with the element of *fire*, which along with earth, water and air made up the elements of Greek cosmology according to Empedocles.† Fire may indeed result in a transition from the gaseous to the plasma state, in which a gas may be fully or, more likely, partially ionized. For the present we identify as *plasma* any state of matter that contains enough free charged particles for its dynamics to be dominated by electromagnetic forces. In practice quite modest degrees of ionization are sufficient for a gas to exhibit electromagnetic properties. Even at 0.1 per cent ionization a gas already has an electrical conductivity almost half the maximum possible, which is reached at about 1 per cent ionization.

The outer layers of the Sun and stars in general are made up of matter in an ionized state and from these regions winds blow through interstellar space contributing, along with stellar radiation, to the ionized state of the interstellar gas. Thus, much of the matter in the Universe exists in the plasma state. The Earth and its lower atmosphere is an exception, forming a plasma-free oasis in a plasma universe. The upper atmosphere on the other hand, stretching into the ionosphere and beyond to the magnetosphere, is rich in plasma effects.

Solar physics and in a wider sense cosmic electrodynamics make up one of the roots from which the physics of plasmas has grown; in particular, that part of the subject known as magnetohydrodynamics – MHD for short – was established largely through the work of Alfvén. A quite separate root developed from the physics of gas discharges, with glow discharges used as light sources and arcs as a means of cutting and welding metals. The word *plasma* was first used by Langmuir in 1928 to describe the ionized regions in gas discharges. These origins

† Empedocles, who lived in Sicily in the shadow of Mount Etna in the fifth century BC, was greatly exercised by fire. He died testing his theory of buoyancy by jumping into the volcano in 433BC.

are discernible even today though the emphasis has shifted. Much of the impetus for the development of plasma physics over the second half of the twentieth century came from research into controlled thermonuclear fusion on the one hand and astrophysical and space plasma phenomena on the other.

To a degree these links with 'big science' mask more bread-and-butter applications of plasma physics over a range of technologies. The use of plasmas as sources for energy-efficient lighting and for metal and waste recycling and their role in surface engineering through high-speed deposition and etching may seem prosaic by comparison with fusion and space science but these and other commercial applications have laid firm foundations for a new plasma technology. That said, our concern throughout this book will focus in the main on the physics of plasmas with illustrations drawn where appropriate from fusion and space applications.

1.2 Thermonuclear fusion

While thermonuclear fusion had been earlier indentified as the source of energy production in stars it was first discussed in detail by Bethe, and independently von Weizsäcker, in 1938. The chain of reactions proposed by Bethe, known as the carbon cycle, has the distinctive feature that after a sequence of thermonuclear burns involving nitrogen and oxygen, carbon is regenerated as an end product enabling the cycle to begin again. For stars with lower central temperatures the proton–proton cycle

$$\begin{aligned} {}_1\mathrm{H}^1 + {}_1\mathrm{H}^1 &\rightarrow {}_1\mathrm{D}^2 + \mathrm{e}^+ + \nu \qquad (1.44\,\mathrm{MeV}) \\ {}_1\mathrm{D}^2 + {}_1\mathrm{H}^1 &\rightarrow {}_2\mathrm{He}^3 + \gamma \qquad (5.49\,\mathrm{MeV}) \\ {}_2\mathrm{He}^3 + {}_2\mathrm{He}^3 &\rightarrow {}_2\mathrm{He}^4 + 2\,{}_1\mathrm{H}^1 \qquad (12.86\,\mathrm{MeV}) \end{aligned}$$

where e^+, ν and γ denote in turn a positron, neutrino and gamma-ray, is more important and is in fact the dominant reaction chain in lower main sequence stars (see Salpeter (1952)). Numbers in brackets denote the energy per reaction. In the first reaction in the cycle, the photon energy released following positron–electron annihilation (1.18 MeV) is included; the balance (0.26 MeV) carried by the neutrino escapes from the star. The third reaction in the cycle is only possible at temperatures above about 10^7 K but accounts for almost half of the total energy release of 26.2 MeV. The proton–proton cycle is dominant in the Sun, the transition to the carbon cycle taking place in stars of slightly higher mass. The energy produced not only ensures stellar stability against gravitational collapse but is the source of luminosity and indeed all aspects of the physics of the outer layers of stars.

The reaction that offers the best energetics for controlled thermonuclear fusion in the laboratory on the other hand is one in which nuclei of deuterium and tritium

fuse to yield an alpha particle and a neutron:

$$_1\mathrm{D}^2 + {}_1\mathrm{T}^3 \rightarrow {}_2\mathrm{He}^4 + {}_0\mathrm{n}^1 \quad (17.6\,\mathrm{MeV})$$

The total energy output $\Delta E = 17.6\,\mathrm{MeV}$ is distributed between the alpha particle which has a kinetic energy of about 3.5 MeV and the neutron which carries the balance of the energy released. The alpha particle is confined by the magnetic field containing the plasma and used to heat the fuel, whereas the neutron escapes through the wall of the device and has to be contained by a neutron-absorbing blanket.

1.2.1 The Lawson criterion

Although the D–T reaction rate peaks at temperatures of the order of 100 keV it is not necessary for reacting nuclei to be as energetic as this, otherwise controlled thermonuclear fusion would be impracticable. Thanks to quantum tunnelling through the Coulomb barrier, the reaction rate for nuclei with energies of the order of 10 keV is sufficiently large for fusion to occur. A simple and widely used index of thermonuclear gain is provided by the Lawson criterion. For equal deuterium and tritium number densities, $n_\mathrm{D} = n_\mathrm{T} = n$, the thermonuclear power generated by a D–T reactor per unit volume is $P_\mathrm{fus} = \frac{1}{4}n^2\langle\sigma v\rangle\Delta E$, where $\langle\sigma v\rangle$ denotes the reaction rate, σ being the collisional cross-section and v the relative velocity of colliding particles. For a D–T plasma at a temperature of 10 keV, $\langle\sigma v\rangle \sim 1.1 \times 10^{-22}\,\mathrm{m^3\,s^{-1}}$ so that $P_\mathrm{fus} \sim 7.7 \times 10^{-35} n^2\,\mathrm{W\,m^{-3}}$. About 20% of this output is alpha particle kinetic energy which is available to sustain the fuel at thermonuclear reaction temperatures, the balance being carried by the neutrons which escape from the plasma. Thus the power absorbed by the plasma is $P_\alpha = \frac{1}{4}\langle\sigma v\rangle n^2 E_\alpha$ where $E_\alpha = 3.5\,\mathrm{MeV}$. This is the heat added to unit volume of plasma per unit time as a result of fusion.

We have to consider next the energy lost through radiation, in particular as bremsstrahlung from electron–ion collisions. We shall find in Chapter 9 that bremsstrahlung power loss from hot plasmas may be represented as $P_\mathrm{b} = \alpha n^2 T^{1/2}$, where α is a constant and T denotes the plasma temperature. Above some critical temperature the power absorbed through alpha particle heating outstrips the bremsstrahlung loss. Other energy losses besides bremsstrahlung have to be taken into consideration. In particular, heat will be lost to the wall surrounding the plasma at a rate $3nk_\mathrm{B}T/\tau$ where τ is the containment time and k_B is Boltzmann's constant. Balancing power gain against loss we arrive at a relation for $n\tau$. Lawson (1957) introduced an efficiency factor η to allow power available for heating to be expressed in terms of the total power leaving the plasma. The *Lawson criterion* for power

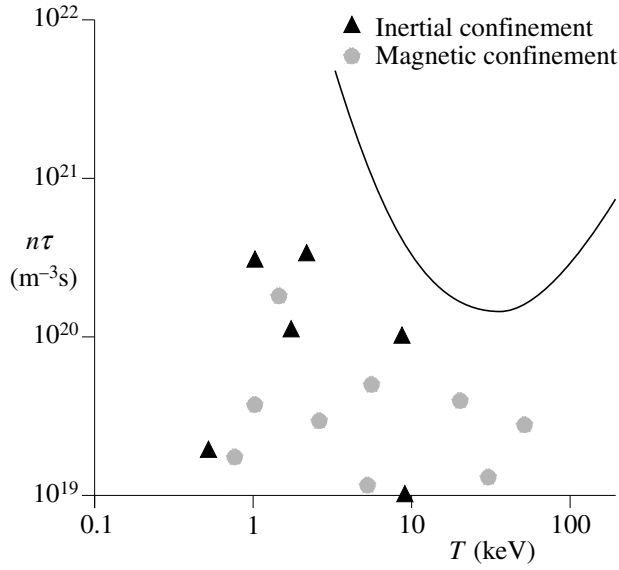

Fig. 1.1. The Lawson criterion for ignition of fusion reactions. Data points correspond to a range of magnetic and inertial confinement experiments showing a progression towards the Lawson curve.

gain is then

$$n\tau > \frac{3k_{\mathrm{B}}T}{\left[\frac{\eta}{4(1-\eta)}\langle\sigma v\rangle\Delta E - \alpha T^{1/2}\right]} \tag{1.1}$$

This condition is represented in Fig. 1.1. Using Lawson's choice for $\eta = 1/3$ (which with hindsight is too optimistic), the power-gain condition reduces to $n\tau > 10^{20}\,\mathrm{m}^{-3}\,\mathrm{s}$. The data points shown in Fig. 1.1 are $n\tau$ values from a range of both magnetically and inertially contained plasmas over a period of about two decades, showing the advances made in both confinement schemes towards the Lawson curve.

1.2.2 Plasma containment

Hot plasmas have to be kept from contact with walls so that from the outset magnetic fields have been used to contain plasma in controlled thermonuclear fusion experiments. Early devices such as Z-pinches, while containing and pinching the plasma radially, suffered serious end losses. Other approaches trapped the plasma in a magnetic bottle or used a closed toroidal vessel. Of the latter the *tokamak*, a contraction of the Russian for *toroidal magnetic chamber*, has been the most successful. Its success compared with competing toroidal containment schemes is

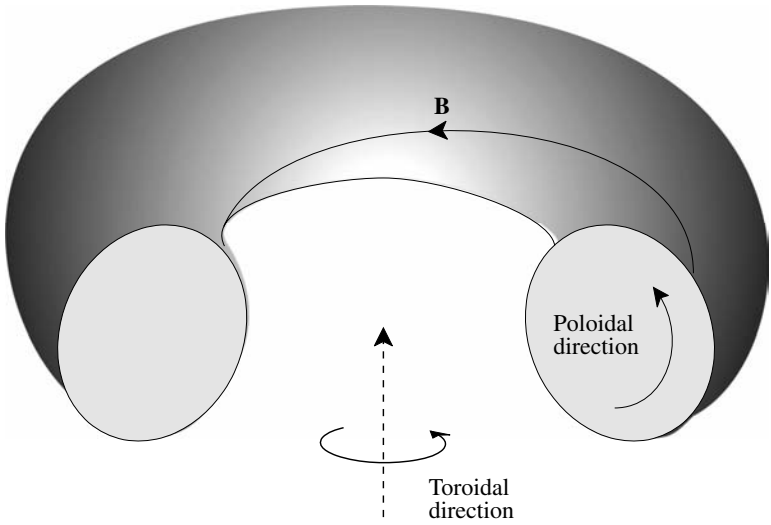

Fig. 1.2. Tokamak cross-section.

attributable in large part to the structure of the magnetic field used. Tokamak fields are made up of two components, one *toroidal*, the other *poloidal*, with the resultant field winding round the torus as illustrated in Fig. 1.2. The toroidal field produced by currents in external coils is typically an order of magnitude larger than the poloidal component and it is this aspect that endows tokamaks with their favourable stability characteristics. Whereas a plasma in a purely toroidal field drifts towards the outer wall, this drift may be countered by balancing the outward force with the magnetic pressure from a poloidal field, produced by currents in the plasma. Broadly speaking, the poloidal field maintains toroidal stability while the toroidal field provides radial stability. For a typical tokamak plasma density the Lawson criterion requires containment times of a few seconds.

Inertial confinement fusion (ICF) offers a distinct alternative to magnetic containment fusion (MCF). In ICF the plasma, formed by irradiating a target with high-power laser beams, is compressed to such high densities that the Lawson criterion can be met for confinement times many orders of magnitude smaller than those needed for MCF and short enough for the plasma to be confined inertially. The ideas behind inertial confinement are represented schematically in Fig. 1.3(a) showing a target, typically a few hundred micrometres in diameter filled with a D–T mixture, irradiated symmetrically with laser light. The ionization at the target surface results in electrons streaming away from the surface, dragging ions in their wake. The back reaction resulting from ion blow-off compresses the target and the aim of inertial confinement is to achieve compression around 1000 times

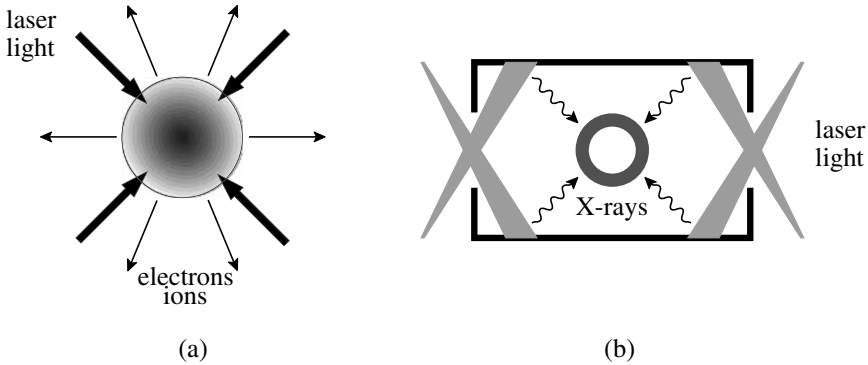

Fig. 1.3. Direct drive (a) and indirect drive (hohlraum) (b) irradiation of targets by intense laser light.

liquid density with minimal heating of the target until the final phase when the compressed fuel is heated to thermonuclear reaction temperatures. An alternative to the *direct drive* approach illustrated in Fig. 1.3(a) is shown in Fig. 1.3(b) in which the target is surrounded by a *hohlraum*. Light enters the hohlraum and produces X-rays which in turn provide target compression and *indirect drive* implosion.

1.3 Plasmas in space

Thermonuclear burn in stars is the source of plasmas in space. From stellar cores where thermonuclear fusion takes place, keV photons propagate outwards towards the surface, undergoing energy degradation through radiation–matter interactions on the way. In the case of the Sun the surface is a black body radiator with a temperature of 5800 K. Photons propagate outwards through the radiation zone across which the temperature drops from about 10^7 K in the core to around 5×10^5 K at the boundary with the convection zone. This boundary is marked by a drop in temperature so steep that radiative transfer becomes unstable and is supplanted as the dominant mode of energy transport by the onset of convection.

Just above the convection zone lies the photosphere, the visible 'surface' of the Sun, in the sense that photons in the visible spectrum escape from the photosphere. UV and X-ray surfaces appear at greater heights. Within the photosphere the Sun's temperature falls to about 4300 K and then unexpectedly begins to rise, a transition that marks the boundary between photosphere and chromosphere. At the top of the chromosphere temperatures reach around 20 000 K and heating then surges dramatically to give temperatures of more than a million degrees in the corona.

The surface of the Sun is characterized by magnetic structures anchored in the photosphere. Not all magnetic field lines form closed loops; some do not close

in the photosphere with the result that plasma flowing along such field lines is not bound to the Sun. This outward flow of coronal plasma in regions of open magnetic field constitutes the solar wind. The interaction between this wind and the Earth's magnetic field is of great interest in the physics of the Sun–Earth plasma system. The Earth is surrounded by an enormous magnetic cavity known as the magnetosphere at which the solar wind is deflected by the geomagnetic field, with dramatic consequences for each. The outer boundary of the magnetosphere occurs at about $10R_{\mathrm{E}}$, where R_{E} denotes the Earth's radius. The geomagnetic field is swept into space in the form of a huge cylinder many millions of kilometres in length, known as the magnetotail. Perhaps the most dramatic effect on the solar wind is the formation of a shock some $5R_{\mathrm{E}}$ upstream of the magnetopause, known as the bow shock. We shall discuss a number of these effects later in the book by way of illustrating basic aspects of the physics of plasmas.

1.4 Plasma characteristics

We now introduce a number of concepts fundamental to the nature of any plasma whatever its origin. First we need to go a step beyond our statement in Section 1.1 and obtain a more formal identification of the plasma condition. Perhaps the most notable feature of a plasma is its ability to maintain a state of charge neutrality. The combination of low electron inertia and strong electrostatic field, which arises from even the slightest charge imbalance, results in a rapid flow of electrons to re-establish neutrality.

The first point to note concerns the nature of the electrostatic field. Although at first sight it might appear that the Coulomb force due to any given particle extends over the whole volume of the plasma, this is in fact not the case. Debye, in the context of electrolytic theory, was the first to point out that the field due to any charge imbalance is shielded so that its influence is effectively restricted to within a finite range. For example, we may suppose that an additional ion with charge Ze is introduced at a point P in an otherwise neutral plasma. The effect will be to attract electrons towards P and repel ions away from P so that the ion is surrounded by a neutralizing 'cloud'. Ignoring ion motion and assuming that the number density of the electron cloud n_{c} is given by the Boltzmann distribution, $n_{\mathrm{c}} = n_{\mathrm{e}} \exp(e\phi/k_{\mathrm{B}}T_{\mathrm{e}})$, where T_{e} is the electron temperature, we solve Poisson's equation for the electrostatic potential $\phi(r)$ in the plasma.

Since $\phi(r) \to 0$ as $r \to \infty$, we may expand $\exp(e\phi/k_{\mathrm{B}}T_{\mathrm{e}})$ and with $Zn_{\mathrm{i}} = n_{\mathrm{e}}$, Poisson's equation for large r and spherical symmetry about P becomes

$$\frac{1}{r^2}\frac{\mathrm{d}}{\mathrm{d}r}\left(r^2\frac{\mathrm{d}\phi}{\mathrm{d}r}\right) = \frac{n_{\mathrm{e}}e^2}{\varepsilon_0 k_{\mathrm{B}}T_{\mathrm{e}}}\phi = \frac{\phi}{\lambda_{\mathrm{D}}^2} \tag{1.2}$$

say, where ε_0 is the vacuum permittivity. Now matching the solution of (1.2), $\phi \sim \exp(-r/\lambda_D)/r$, with the potential $\phi = Ze/4\pi\varepsilon_0 r$ as $r \to 0$ we see that

$$\phi(r) = \frac{Ze}{4\pi\varepsilon_0 r} \exp(-r/\lambda_D) \tag{1.3}$$

where

$$\lambda_D = \left(\frac{\varepsilon_0 k_B T_e}{n_e e^2}\right)^{1/2} \simeq 7.43 \times 10^3 \left(\frac{T_e(\text{eV})}{n_e}\right)^{1/2} \text{ m} \tag{1.4}$$

is called the *Debye shielding length*. Beyond a *Debye sphere*, a sphere of radius λ_D, centred at P, the plasma remains effectively neutral. By the same argument λ_D is also a measure of the penetration depth of external electrostatic fields, i.e. of the thickness of the boundary sheath over which charge neutrality may not be maintained.

The plausibility of the argument used to establish (1.3) requires that a large number of electrons be present within the Debye sphere, i.e. $n_e\lambda_D^3 \gg 1$. The inverse of this number is proportional to the ratio of potential energy to kinetic energy in the plasma and may be expressed as

$$g = \frac{e^2}{\varepsilon_0 k_B T_e \lambda_D} = \frac{1}{n_e \lambda_D^3} \ll 1 \tag{1.5}$$

Since g plays a key role in the development of formal plasma theory it is known as the *plasma parameter*. Broadly speaking, the more particles there are in the Debye sphere the less likely it is that there will be a significant resultant force on any given particle due to 'collisions'. It is, therefore, a measure of the dominance of collective interactions over collisions.

The most fundamental of these collective interactions are the *plasma oscillations* set up in response to a charge imbalance. The strong electrostatic fields which drive the electrons to re-establish neutrality cause oscillations about the equilibrium position at a characteristic frequency, the *plasma frequency* ω_p. Since the imbalance occurs over a distance λ_D and the electron thermal speed V_e is typically $(k_B T_e/m_e)^{1/2}$ we may express the electron plasma frequency ω_{pe} by

$$\omega_{pe} = \frac{(k_B T_e/m_e)^{1/2}}{\lambda_D} = \left(\frac{n_e e^2}{m_e \varepsilon_0}\right)^{1/2} \tag{1.6}$$

which reduces to $\omega_{pe} \simeq 56.4 n_e^{1/2}\,\mathrm{s}^{-1}$. Note that any applied fields with frequencies less than the electron plasma frequency are prevented from penetrating the plasma by the more rapid electron response which neutralizes the field. Thus a plasma is not transparent to electromagnetic radiation of frequency $\omega < \omega_{pe}$. The corresponding frequency for ions, the *ion plasma frequency* ω_{pi}, is defined by

$$\omega_{pi} = \left(\frac{n_i (Ze)^2}{m_i \varepsilon_0}\right)^{1/2} \simeq 1.32 Z \left(\frac{n_i}{A}\right)^{1/2} \tag{1.7}$$

where Z denotes the charge state and A the atomic number.

1.4.1 Collisions and the plasma parameter

We have seen that the effective range of an electric field, and hence of a collision, is the Debye length λ_D. Thus any particle interacts at any instant with the large number of particles in its Debye sphere. Plasma collisions are therefore *many-body interactions* and since $g \ll 1$ collisions are predominantly weak, in sharp contrast with the strong, binary collisions that characterize a neutral gas. In gas kinetics a collision frequency ν_c is defined by $\nu_c = n V_{th} \sigma(\pi/2)$ where $\sigma(\pi/2)$ denotes the cross-section for scattering through $\pi/2$ and V_{th} is a thermal velocity. Such a deflection in a plasma would occur for particles 1 and 2 interacting over a distance b_0 for which $e_1 e_2 / 4\pi\varepsilon_0 b_0 \sim k_B T$ so that $\nu_c = (n V_{th} \pi b_0^2)$. However, the cumulative effect of the much more frequent weak interactions acts to increase this by a factor $\sim 8 \ln(\lambda_D / b_0) \approx 8 \ln(4\pi n \lambda_D^3)$. For electron collisions with ions of charge Ze it follows that the electron–ion collision time $\tau_{ei} \equiv \nu_{ei}^{-1}$ is given by

$$\tau_{ei} = \frac{2\pi \varepsilon_0^2 m_e^{1/2} (k_B T_e)^{3/2}}{Z^2 n_i e^4 \ln \Lambda} \tag{1.8}$$

where $\ln \Lambda = \ln 4\pi n \lambda_D^3$ is known as the *Coulomb logarithm*. For singly charged ions the electron–ion collision time is

$$\tau_{ei} = 3.44 \times 10^{11} \frac{T_e^{3/2}\,(\mathrm{eV})}{n_i \ln \Lambda}\ \mathrm{s}$$

in which we have replaced the factor 2π in (1.8) with the value found from a correct treatment of plasma transport in Chapter 12. The Coulomb logarithm is

$$\ln \Lambda = 6.6 - \frac{1}{2} \ln\left(\frac{n}{10^{20}}\right) + \frac{3}{2} \ln T_e\,(\mathrm{eV})$$

The *electron mean free path* $\lambda_e = V_e \tau_{ei}$ is

$$\lambda_e = 1.44 \times 10^{17} \frac{T_e^2 (\mathrm{eV})}{n_i \ln \Lambda}$$

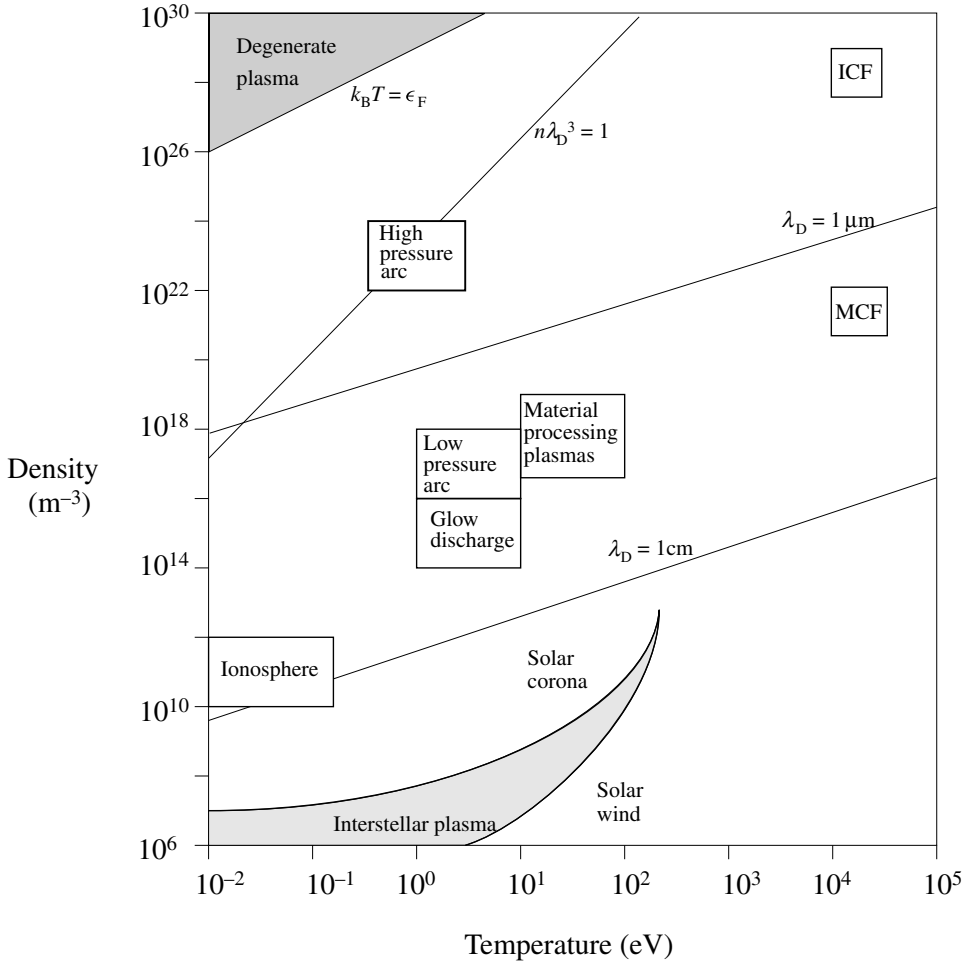

Fig. 1.4. Landmarks in the plasma universe.

Table 1.1 lists approximate values of various plasma parameters along with typical values of the magnetic field associated with each for a range of plasmas across the plasma universe. These and other representative plasmas are included in the diagram of parameter space in Fig. 1.4 which includes the parameter lines $\lambda_D = 1\,\mu m$, 1 cm and $n\lambda_D^3 = 1$ together with the line marking the boundary at which plasmas become degenerate $k_B T = \epsilon_F$, where ϵ_F denotes the Fermi energy.

Table 1.1. *Approximate values of parameters across the plasma universe.*

Plasma	n (m^{-3})	T (keV)	B (T)	ω_{pe} (s^{-1})	λ_D (m)	$n\lambda_D^3$	ν_{ei} (Hz)
Interstellar	10^6	10^{-5}	10^{-9}	$6 \cdot 10^4$	0.7	$3 \cdot 10^5$	$4 \cdot 10^8$
Solar wind (1 AU)	10^7	10^{-2}	10^{-8}	$2 \cdot 10^5$	7	$4 \cdot 10^9$	10^{-4}
Ionosphere	10^{12}	10^{-4}	10^{-5}	$6 \cdot 10^7$	$2 \cdot 10^{-3}$	10^4	10^4
Solar corona	10^{12}	0.1	10^{-3}	$6 \cdot 10^7$	0.07	$4 \cdot 10^8$	0.5
Arc discharge	10^{20}	10^{-3}	0.1	$6 \cdot 10^{11}$	$7 \cdot 10^{-7}$	40	10^{10}
Tokamak	10^{20}	10	10	$6 \cdot 10^{11}$	$7 \cdot 10^{-5}$	$3 \cdot 10^7$	$4 \cdot 10^4$
ICF	10^{28}	10	—	$6 \cdot 10^{15}$	$7 \cdot 10^{-9}$	$4 \cdot 10^3$	$4 \cdot 10^{11}$

2

Particle orbit theory

2.1 Introduction

On the face of it, solving an equation of motion to determine the orbit of a single charged particle in prescribed electric and magnetic fields may not seem like the best way of going about developing the physics of plasmas. Given the central role of collective interactions hinted at in Chapter 1 and the subtle interplay of currents and fields that will be explored in the chapters on MHD that follow, it is at least worth asking "Why bother with orbit theory?". One attraction is its relative simplicity. Beyond that, key concepts in orbit theory prove useful throughout plasma physics, sometimes shedding light on other plasma models.

Before developing particle orbit theory it is as well to be clear about conditions under which this description might be valid. Intuitively we expect orbit theory to be useful in describing the motion of high energy particles in low density plasmas where particle collisions are infrequent. More specifically, we need to make sure that the effect of self-consistent fields from neighbouring charges is small compared with applied fields. Then if we want to solve the equation of motion analytically the fields in question need to show a degree of symmetry. We shall find that scaling associated with an applied magnetic field is one reason – indeed the principal reason – for the success of orbit theory. Particle orbits in a magnetic field define both a natural length, r_{L}, the particle Larmor radius, and frequency, Ω, the cyclotron frequency. For many plasmas these are such that the scale length, L, and characteristic time, T, of the physics involved satisfy an ordering $r_{\mathrm{L}}/L \ll 1$ and $2\pi/\Omega T \ll 1$. This natural ordering lets us solve the dynamical equations in inhomogeneous and time-dependent fields by making perturbation expansions using r_{L}/L and $2\pi/\Omega T$ as small parameters. In this way Alfvén showed that one could filter out the rapid gyro-motion about magnetic field lines and focus on the dynamics of the centre of this motion, the so-called guiding centre. Alfvén's guiding centre model and the concept of adiabatic invariants (quantities that are

not exact constants of the motion but, in certain circumstances, nearly so) play a key role in orbit theory. In large part, this chapter is taken up with the development and application of Alfvén's ideas.

Throughout this chapter we shall assume that radiative effects are negligible. For the present we suppose that particle energies are such that we need only solve the non-relativistic Lorentz equation for the motion of a particle of mass m_j and charge e_j at a position $\mathbf{r}_j(t)$ moving in an electric field $\mathbf{E}$ and a magnetic field $\mathbf{B}$

$$m_j \ddot{\mathbf{r}}_j = e_j \left[\mathbf{E}(\mathbf{r}, t) + \dot{\mathbf{r}}_j \times \mathbf{B}(\mathbf{r}, t) \right] \tag{2.1}$$

under prescribed initial conditions. This needs to be done for particles of each species. An important part of this procedure requires checking for self-consistency of the assumed fields. For the most part this means ensuring that fields induced by the motion of particles are negligible compared with the applied fields. For this we use Maxwell's equations

$$\nabla \times \mathbf{E} = -\frac{\partial \mathbf{B}}{\partial t} \tag{2.2}$$

$$\nabla \times \mathbf{B} = \varepsilon_0 \mu_0 \frac{\partial \mathbf{E}}{\partial t} + \mu_0 \mathbf{j} \tag{2.3}$$

$$\nabla \cdot \mathbf{E} = q/\varepsilon_0 \tag{2.4}$$

$$\nabla \cdot \mathbf{B} = 0 \tag{2.5}$$

in which $\mathbf{j}(\mathbf{r}, t)$ and $q(\mathbf{r}, t)$ are current and charge densities defined by

$$\mathbf{j}(\mathbf{r}, t) = \sum_{j=1}^{N} e_j \dot{\mathbf{r}}_j(t) \delta(\mathbf{r} - \mathbf{r}_j(t)) \tag{2.6}$$

$$q(\mathbf{r}, t) = \sum_{j=1}^{N} e_j \delta(\mathbf{r} - \mathbf{r}_j(t)) \tag{2.7}$$

where δ denotes the Dirac delta function and sums are taken over *all* plasma particles. Checking for self-consistency, though not often stressed, is important since it may impose limits on the use of orbit theory and, in some cases, necessary conditions on the plasma or fields which would not otherwise be obvious. In the following applications of orbit theory we discuss self-consistency only when it gives rise to such limitations. In general whenever charge distributions or current densities are significant, orbit theory is no longer adequate and statistical or fluid descriptions are then essential.

2.2 Constant homogeneous magnetic field

The simplest problem in orbit theory is that of the non-relativistic motion of a charged particle in a constant, spatially uniform magnetic field, $\mathbf{B}$, with $\mathbf{E} = 0$. Moreover, we shall see that it is straightforward to deal with more general cases as perturbations of this basic motion. For simplicity of notation we discard the subscript j on e_j and m_j except where we wish specifically to distinguish between ions and electrons. Taking the direction of $\mathbf{B}$ to define the z-axis, that is $\mathbf{B} = B\hat{\mathbf{z}}$, the scalar product of (2.1) with $\hat{\mathbf{z}}$ gives,

$$\ddot{z} = 0 \tag{2.8}$$

so that $\dot{z} = v_\parallel = \text{ const.}$ Also from (2.1),

$$m\ddot{\mathbf{r}} \cdot \dot{\mathbf{r}} = 0$$

so that

$$\tfrac{1}{2}m\dot{r}^2 = W = \text{ const.}$$

Hence the magnitude of velocity components both perpendicular ($v_\perp$) and parallel ($v_\parallel$) to $\mathbf{B}$ are constant and the kinetic energy

$$W = W_\perp + W_\parallel = \tfrac{1}{2}m(v_\perp^2 + v_\parallel^2)$$

It is no surprise that kinetic energy is conserved since the force is always perpendicular to the velocity of the particle and, in consequence, does no work on it. Moreover, conservation of kinetic energy is not restricted to uniform magnetic fields.

The particle trajectory is determined by (2.8) together with the x and y components of (2.1):

$$\ddot{x} = \Omega\dot{y} \qquad \ddot{y} = -\Omega\dot{x}$$

where $\Omega = eB/m$. A convenient way of dealing with motion transverse to $\mathbf{B}$ starts by defining $\zeta = x + iy$ so that

$$\ddot{\zeta} + i\Omega\dot{\zeta} = 0$$

Integrating once with respect to time gives

$$\dot{\zeta}(t) = \dot{\zeta}(0)\exp(-i\Omega t)$$

and by defining $\dot{\zeta}(0) = v_\perp \exp(-i\alpha)$ it follows that

$$\dot{x} = v_\perp \cos(\Omega t + \alpha) \qquad \dot{y} = -v_\perp \sin(\Omega t + \alpha) \tag{2.9}$$

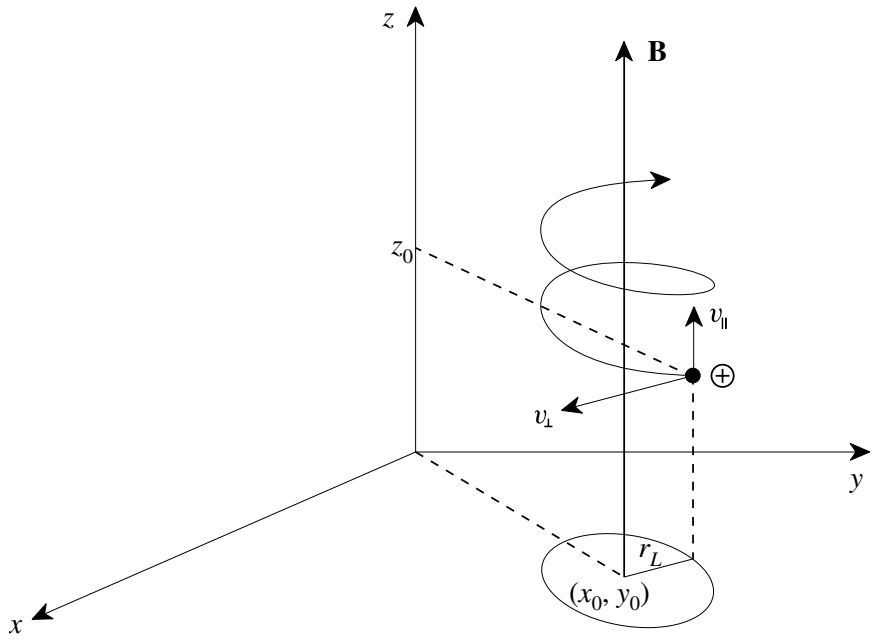

Fig. 2.1. Orbit of a positively charged particle in a uniform magnetic field.

Integrating a second time determines the particle orbit

$$\left.\begin{aligned} x &= \left(\frac{v_\perp}{\Omega}\right)\sin(\Omega t+\alpha)+x_0 \\ y &= \left(\frac{v_\perp}{\Omega}\right)\cos(\Omega t+\alpha)+y_0 \end{aligned}\right\} \tag{2.10}$$

and

$$z = v_\parallel t + z_0 \tag{2.11}$$

where α, x_0, y_0, and z_0, together with $v_\perp$ and $v_\parallel$, are determined by the initial conditions. The quantity $\phi(t) \equiv (\Omega t + \alpha)$ is sometimes referred to as the *gyro-phase*. The superposition of uniform motion in the direction of the magnetic field on the circular orbits in the plane normal to **B** defines a helix of constant pitch with axis parallel to **B** as shown in Fig. 2.1 for a positively charged particle. Referred to the moving plane $z = v_\parallel t + z_0$ the orbit projects as a circle with centre (x_0, y_0) and radius $r_\mathrm{L} = v_\perp/|\Omega|$. The centre of this circle, known as the *guiding centre*, describes the locus $\mathbf{r}_\mathrm{g} = (x_0, y_0, v_\parallel t + z_0)$. It is important to emphasize that the guiding centre is not the locus of a particle as such. The radius of the circle, r_L, is known as the *Larmor radius* and the frequency of rotation, Ω, as the *Larmor frequency*, *cyclotron frequency*, or *gyro-frequency*. The sense of rotation for a

prescribed magnetic field is determined by Ω which depends on the sign of the charge. Viewed from $z = +\infty$, positive and negative particles rotate in clockwise and anticlockwise directions, respectively. For electrons $|\Omega_e| = 1.76 \times 10^{11}\, B\ \mathrm{s}^{-1}$, while for protons $\Omega_p = 9.58 \times 10^7\, B\ \mathrm{s}^{-1}$ where B is measured in teslas. In many applications of orbit theory we need concern ourselves only with guiding centre motion. However aspects of the Larmor motion are needed for discussion later in the chapter and we next look briefly at one of these.

2.2.1 Magnetic moment and plasma diamagnetism

We can formally associate a microscopic current I_L with the Larmor motion. The magnetic field from this microcurrent is determined by Ampère's law and is oppositely directed to the applied magnetic field. In this sense the response of the particle to the magnetic field is *diamagnetic*. In the same formal sense we may associate with this microcurrent a *magnetic moment* $\boldsymbol{\mu}_B$ given by

$$\boldsymbol{\mu}_B = -\pi r_L^2 I_L \mathbf{B}/|\mathbf{B}| = -\pi r_L^2 \left(\frac{e\Omega}{2\pi}\right) \frac{\mathbf{B}}{|\mathbf{B}|}$$

where $2\pi/|\Omega|$ is a Larmor period. From this it follows that

$$\boldsymbol{\mu}_B = -\frac{W_\perp}{B^2}\mathbf{B}$$

If we now extend this argument to all plasma particles we can find an expression for the magnetization per unit volume by summing individual moments over the distribution of particles. For n particles per unit volume the magnetization $\mathbf{M} = n\langle\boldsymbol{\mu}_B\rangle$ where the brackets denote an average. Then using $\mathbf{j}_M = \boldsymbol{\nabla} \times \mathbf{M} = \mu_0^{-1}\boldsymbol{\nabla} \times \mathbf{B}_{ind}$, the magnitude of the induced field B_{ind} relative to the applied magnetic field is

$$\frac{B_{ind}}{B} \sim \frac{\mu_0 n \langle W_\perp \rangle}{B^2}$$

where $\langle W_\perp \rangle$ denotes the average kinetic energy perpendicular to $\mathbf{B}$. Since we require the induced field to be small compared with the applied field this implies that the kinetic energy of the plasma must be much less than the magnetic energy.

2.3 Constant homogeneous electric and magnetic fields

We now introduce a constant, uniform electric field which may be resolved into components $\mathbf{E}_\parallel$ in the direction of $\mathbf{B}$ and $\mathbf{E}_\perp$, which is taken to define the direction

of the y-axis. Thus $\mathbf{B} = (0, 0, B)$, $\mathbf{E} = (0, E_\perp, E_\parallel)$, and the components of (2.1) are

$$\ddot{x} = \Omega\dot{y} \tag{2.12}$$

$$\ddot{y} = \frac{eE_\perp}{m} - \Omega\dot{x} \tag{2.13}$$

$$\ddot{z} = \frac{eE_\parallel}{m} \tag{2.14}$$

Integrating (2.14) once gives

$$\dot{z} = v_\parallel + \frac{eE_\parallel t}{m}$$

from which it is clear that for sufficiently long times the non-relativistic approximation breaks down unless $E_\parallel = 0$. Further, since charges of opposite sign are accelerated in opposite directions, a non-zero $E_\parallel$ gives rise to arbitrarily large currents and charge separation. Therefore, from (2.3) and (2.4) significant fluctuating fields are induced contrary to our assumption of constant fields. Thus for consistency it is necessary to set $E_\parallel = 0$ in this approximation.

Equations (2.12) and (2.13) are solved as in Section 2.2. Now

$$\ddot{\zeta} + i\Omega\dot{\zeta} = \frac{ieE}{m} \tag{2.15}$$

where $E_\perp$ has been replaced by E. Integrating once gives

$$\dot{\zeta}(t) = \dot{\zeta}(0)e^{-i\Omega t} + v_\mathrm{E}(1 - e^{-i\Omega t})$$

where $v_\mathrm{E} = E/B$. Hence

$$\dot{x} = u\cos(\Omega t + \alpha) + v_\mathrm{E} \qquad \dot{y} = -u\sin(\Omega t + \alpha)$$

where u and α are constants defined by

$$\dot{\zeta}(0) - v_\mathrm{E} = ue^{-i\alpha}$$

The velocity of the guiding centre is now

$$\mathbf{v}_\mathrm{g} = (v_\mathrm{E}, 0, v_\parallel)$$

Thus the effect of an electric field perpendicular to the magnetic field is to produce a drift orthogonal to both. This means that the guiding centre is no longer tied to a particular field line but drifts across field lines. The drift velocity, which may be written

$$\mathbf{v}_\mathrm{E} = (\mathbf{E} \times \mathbf{B})/B^2 \tag{2.16}$$

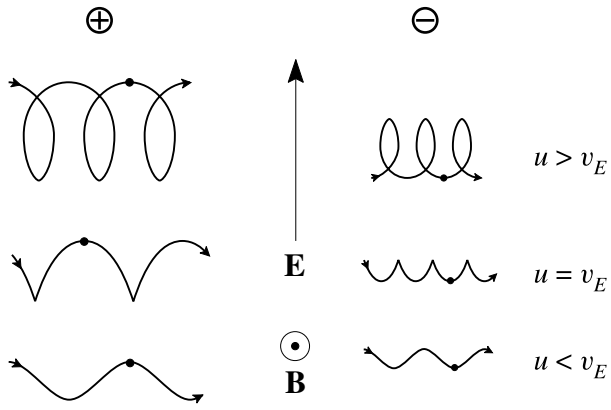

Fig. 2.2. Drift produced by a constant uniform electric field perpendicular to the magnetic field.

depends only on the fields; in particular, being independent of particle charge it cannot give rise to a current. The non-relativistic approximation implies a further restriction on the electric field; by (2.16), $E \ll cB$, where c is the speed of light. The trajectories of positive and negative particles in the plane defined by (2.11), found from a second integration of (2.15), are shown in Fig. 2.2. In its Larmor cycle a positive charge slows when moving in opposition to the electric field and accelerates when moving with it. Thus the Larmor orbit is continuously distorted as the instantaneous Larmor radius alternately becomes shorter in one half-cycle and longer in the next as in Fig. 2.2. The net effect is a drift to the right. The electrons also drift to the right since the opposite action of the field is compensated for by the anti-clockwise rotation. The mass difference between positively and negatively charged particles is represented schematically in Fig. 2.2 by the smaller electron drift per cycle which is fully compensated by the proportionately bigger Larmor frequency.

2.3.1 Constant non-electromagnetic forces

It may happen that the particles are subject to non-electromagnetic forces such as gravity. If such a force, $\mathbf{F}$, is constant it is equivalent to an electric field $\mathbf{E}' = \mathbf{F}/e$ and is subject to the same restrictions found for $\mathbf{E}$, i.e. its component parallel to $\mathbf{B}$ must be negligible and $F \ll ceB$. The drift velocity is then

$$\mathbf{v}_{\mathrm{F}} = (\mathbf{F} \times \mathbf{B})/eB^2$$

In contrast to $\mathbf{v}_{\mathrm{E}}$ this drift contributes to a current. There is a nice antithesis here in that a non-electromagnetic drift produces a current whereas the electromagnetic

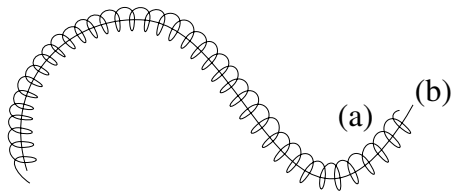

Fig. 2.3. Particle motion showing (a) exact and (b) guiding centre trajectories.

drift $\mathbf{v}_E$ does not. Note that drifts from gravitational forces while usually insignificant in laboratory plasmas normally need to be taken into account when applying orbit theory in space plasmas.

2.4 Inhomogeneous magnetic field

In practice the fields we encounter are generally both space- and time-dependent. Restricting ourselves for the present to spatially inhomogeneous magnetic fields, $\mathbf{B}(\mathbf{r})$, it is necessary to solve (2.1) numerically in general. However, if the inhomogeneity is small – that is, the field experienced by the particle in traversing a Larmor orbit is almost constant – it is possible to determine the trajectory as a perturbation of the basic motion found in Section 2.2. With $\mathbf{B}(\mathbf{r}) \simeq \mathbf{B}(\mathbf{r}_0) + (\delta\mathbf{r} \cdot \boldsymbol{\nabla})\mathbf{B}|_{\mathbf{r}=\mathbf{r}_0}$, where $\mathbf{r}_0$ is the instantaneous position of the guiding centre and $\delta\mathbf{r} = \mathbf{r} - \mathbf{r}_0$, we require that $\delta\mathbf{B}$, the change in $\mathbf{B}$ over a distance r_L, be such that

$$|\delta\mathbf{B}| = |(\delta\mathbf{r} \cdot \boldsymbol{\nabla})\mathbf{B}| \ll |\mathbf{B}|$$

i.e. $r_L \ll L$ where L is a distance over which the field changes significantly.

This perturbation approach was first applied systematically by Alfvén. It is known as the *guiding centre approximation* and has proved a robust tool in the application of orbit theory to cases of practical interest. Alfvén recognized that in many such applications one need not bother with the fast Larmor motion which can be averaged out to leave the slower guiding centre motion illustrated in Fig. 2.3.

The most general inhomogeneous field represented by the nine components of $[\partial B_i/\partial x_j]$ gives rise to distinct kinds of drift from the *gradient* and *curvature* terms. We look at each of these in turn.

2.4.1 Gradient drift

Taking $\mathbf{B} = (0, 0, B(y))$ and $\mathbf{E} = 0$, (2.1) gives

$$\ddot{x} = \Omega(y)\dot{y} \qquad \ddot{y} = -\Omega(y)\dot{x}$$

so that

$$\ddot{\zeta} = -i\Omega(y)\dot{\zeta} \tag{2.17}$$

and

$$\ddot{z} = 0 \tag{2.18}$$

With the assumption $\delta B \ll B$, Ω may be expanded about the initial position of the guiding centre to give

$$\Omega(y) \simeq \Omega(y_0) + (y - y_0)\left.\frac{\mathrm{d}\Omega}{\mathrm{d}y}\right|_{y_0} = \Omega_0 + (y - y_0)\Omega_0'$$

Hence

$$\ddot{\zeta} + i\Omega_0\dot{\zeta} = -i\Omega_0'(y - y_0)\dot{\zeta} \tag{2.19}$$

The terms on the left are zero-order while that on the right is first-order and, as such, y and $\dot{\zeta}$ may be replaced by their zero-order (that is, uniform **B**) values from (2.9) and (2.10) giving

$$\ddot{\zeta} + i\Omega_0\dot{\boldsymbol{\zeta}} = -i\Omega_0'\frac{v_\perp^2}{\Omega_0}\cos(\Omega_0 t + \alpha)e^{-i(\Omega_0 t + \alpha)}$$

On integrating once

$$\dot{\zeta}(t) = \dot{\zeta}(0)e^{-i\Omega_0 t} - \frac{i\Omega_0' v_\perp^2}{\Omega_0^2}e^{-i(\Omega_0 t + \alpha)}[\sin(\Omega_0 t + \alpha) - \sin\alpha]$$

Then

$$\dot{x}(t) = v_\perp\cos(\Omega_0 t + \alpha) - \frac{\Omega_0' v_\perp^2}{2\Omega_0^2}[1 - \cos 2(\Omega_0 t + \alpha) - 2\sin(\Omega_0 t + \alpha)\sin\alpha] \tag{2.20}$$

$$\dot{y}(t) = -v_\perp\sin(\Omega_0 t + \alpha) - \frac{\Omega_0' v_\perp^2}{2\Omega_0^2}[\sin 2(\Omega_0 t + \alpha) - 2\cos(\Omega_0 t + \alpha)\sin\alpha] \tag{2.21}$$

These solutions satisfy identical initial conditions to the uniform **B** case. Also, from (2.18) $\dot{z} = v_\parallel$. From (2.20) and (2.21) we see that oscillations occur at $2\Omega_0$ in addition to those at Ω_0. In the present context, however, the term of interest is the non-oscillatory one in (2.20). The average of the velocity over one period ($T = 2\pi/\Omega_0$) is

$$\langle\mathbf{v}\rangle = (-v_\perp^2\Omega_0'/2\Omega_0^2, 0, v_\parallel)$$

Thus a magnetic field in the z direction with a gradient in the y direction gives rise to a drift in the x direction. This *grad B drift velocity* may be written

$$\mathbf{v}_\mathrm{G} = [W_\perp(\mathbf{B}\times\boldsymbol{\nabla})B]/eB^3 \tag{2.22}$$

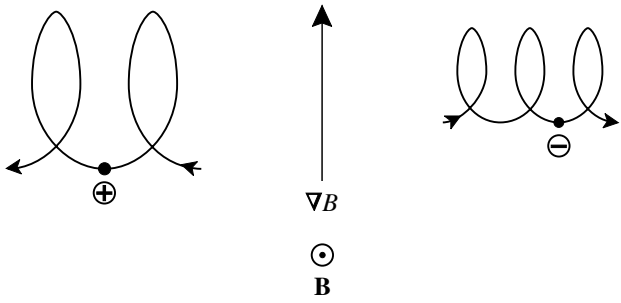

Fig. 2.4. Drift produced by an inhomogeneous magnetic field.

In this case, the drift depends on properties of the particle and, in particular, occurs in opposite directions for positive and negative charges. However, this of itself does not imply a flow of current as we shall see in Section 2.5. The physical source of the ∇B drift is clear from Fig. 2.4 which shows the Larmor radius bigger in regions of weaker $\mathbf{B}$. Thus there will be a drift perpendicular both to $\mathbf{B}$ and ∇B but in this case the opposite rotation of positive and negative charges leads to drifts in opposite directions.

2.4.2 Curvature drift

In practice magnetic fields not only vary spatially but are generally curved and the curvature of field lines in turn gives rise to a drift. For example, if $\mathbf{B} = (0, B_y(z), B)$, where B_y and $\mathrm{d}B_y/\mathrm{d}z$ are taken as small quantities,† one has

$$\ddot{x} = \Omega\dot{y} - \Omega_y\dot{z} \qquad \ddot{y} = -\Omega\dot{x} \qquad \ddot{z} = \Omega_y\dot{x}$$

where $\Omega_y = (eB_y/m)$. Hence,

$$\ddot{\zeta} + i\Omega\dot{\zeta} = -\Omega_y(z)\dot{z} = -\Omega_y(z)v_\parallel$$

neglecting squares of small quantities. It is straightforward to show that there is a drift in the x-direction given by

$$v_\mathrm{C} = \langle\dot{x}\rangle = -v_\parallel^2\Omega_y'/\Omega^2 = -mv_\parallel^2(\mathrm{d}B_y/\mathrm{d}z)/eB^2$$

This *curvature drift velocity* may be written more generally

$$\mathbf{v}_\mathrm{C} = 2W_\parallel(\mathbf{B}\times(\mathbf{B}\cdot\nabla)\mathbf{B})/eB^4 \tag{2.23}$$

† It is convenient to keep B for the z component of $\mathbf{B}$. Since $|\mathbf{B}|$ does not appear in the remainder of this section no confusion arises.

There is also a drift in the y-direction given by $(v_\parallel \Omega_y/\Omega)$. This merely keeps the guiding centre moving parallel to $\mathbf{B}$ in the Oyz-plane since, on average,

$$\frac{\langle \dot{y} \rangle}{\langle \dot{z} \rangle} = \frac{v_\parallel \Omega_y/\Omega}{v_\parallel} = \frac{B_y}{B}$$

To see the physical origin of the curvature drift, picture the particle moving along a curved field line with velocity $v_\parallel$. Because of the curvature the particle will feel a centrifugal force $\mathbf{F} = m v_\parallel^2 \mathbf{R}_c / R_c^2$ where $\mathbf{R}_c$ is a vector from the local centre of curvature to the position of the charge. From Section 2.3.1, $\mathbf{v}_F = (\mathbf{F} \times \mathbf{B})/eB^2$ and so

$$\mathbf{v}_C = \frac{m v_\parallel^2}{eB^2} \frac{\mathbf{R}_c \times \mathbf{B}}{R_c^2}$$

Since the magnetic field lines are defined by $\mathrm{d}\mathbf{l} \times \mathbf{B} = 0$ so that $\mathrm{d}y/B_y = \mathrm{d}z/B$, it follows that $R_c^{-1} \simeq \mathrm{d}^2 y/\mathrm{d}z^2 \simeq B^{-1}\, \mathrm{d}B_y/\mathrm{d}z$. Hence

$$v_C = -m v_\parallel^2 (\mathrm{d}B_y/\mathrm{d}z)/eB^2$$

If the magnetic field is characterized by both gradient and curvature terms in $\nabla \mathbf{B}$ and there are no currents present so that $\nabla \times \mathbf{B} = 0$, then $\partial B_y/\partial z = \partial B/\partial y$ and the total drift velocity is given by

$$\mathbf{v}_B = [(W_\perp + 2W_\parallel)(\mathbf{B} \times \nabla) B]/eB^3 \tag{2.24}$$

Taken together these drifts describe completely the lowest order motion of the guiding centre across an inhomogeneous time-independent magnetic field. The drift velocities are $O(r_L/L)$ times the particle velocities.

Of the other possible inhomogeneities in the magnetic field, the divergence terms are considered in Section 2.6.1. However neither these, nor either of the remaining components of $[\partial B_i/\partial x_j]$ describing shear, give rise to drift motion.

2.5 Particle drifts and plasma currents

We have already sounded a note of caution about too readily identifying particle guiding centre drifts with plasma current. A current density properly involves an average over a distribution of particles, a procedure that makes no direct appeal to the guiding centre motion of particles. Guiding centre drifts on the other hand are found from time-averaging the motion of a single particle. There are no grounds for supposing the two averages are identical and in general they are not.

Let us form a current density corresponding to the ∇B drift from (2.22) by summing over ions (i) and electrons (e) and using $\langle W_\perp \rangle$ to denote average values of $W_\perp$ (cf. Section 2.2.1). Then

$$\begin{aligned} \mathbf{j}_G &= (n_i \langle W_{\perp i} \rangle + n_e \langle W_{\perp e} \rangle) \mathbf{B} \times \nabla B / B^3 \\ &= [n \langle W_\perp \rangle (\mathbf{B} \times \nabla B)] / B^3 \end{aligned} \tag{2.25}$$

To arrive at the total current density we must remember to include the contribution from the plasma diamagnetism. In Section 2.2.1 we saw that the magnetization per unit volume of plasma, $\mathbf{M}$, is given by

$$\mathbf{M} = -\frac{n \langle W_\perp \rangle}{B^2} \mathbf{B}$$

from which the magnetization current density is

$$\mathbf{j}_M = -\nabla \times \left(\frac{n \langle W_\perp \rangle}{B^2} \mathbf{B} \right) \tag{2.26}$$

The total current density is then the sum of $\mathbf{j}_G$ and $\mathbf{j}_M$; for simplicity we suppose there is no field curvature.

If we now turn to the configuration of Section 2.4.1 with $\mathbf{B} = (0, 0, B(y))$ we find that part of the magnetization current density cancels the contribution from the field gradient, so that

$$j_x = (\mathbf{j}_G + \mathbf{j}_M) \cdot \hat{\mathbf{x}} = -\frac{n \langle W_\perp \rangle}{B^2} \frac{dB}{dy} - \frac{d}{dy} \left[\frac{n \langle W_\perp \rangle}{B} \right] = -\frac{1}{B} \frac{d}{dy} (n \langle W_\perp \rangle) \tag{2.27}$$

The effects of plasma magnetization and guiding centre drift in an inhomogeneous magnetic field combine to produce a current perpendicular both to the magnetic field and to the direction in which the field varies, provided $n \langle W_\perp \rangle$ is spatially non-uniform. If we now substitute (2.27) into (2.3) we find, neglecting displacement current,

$$\left[\frac{dB}{dy} + \frac{\mu_0}{B} \frac{d}{dy} (n \langle W_\perp \rangle) \right] = 0 \tag{2.28}$$

so that $n \langle W_\perp \rangle + B^2 / 2\mu_0 = \text{const}$. Thus we see that our picture is consistent only if the increasing magnetic field is compensated by a corresponding decrease in $n \langle W_\perp \rangle$ (or as we shall see in Section 3.4.2, by decreasing pressure). The particular case of decreasing density is illustrated in Fig. 2.5.

In general if one keeps the displacement current term in Maxwell's equations there is then a time-dependent electric field which gives rise to plasma oscillations. Any appeal to orbit theory in conditions where charge separation is significant is of doubtful value. However, if the time dependence of the electric field is slow enough

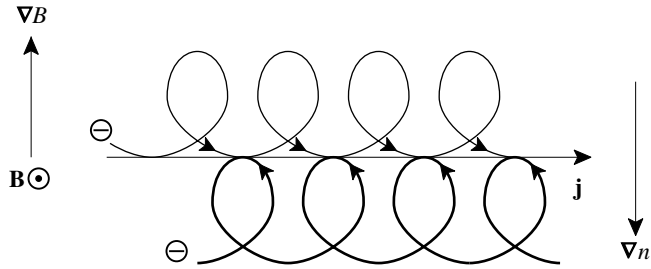

Fig. 2.5. Current density in an inhomogeneous magnetized plasma. In any current sheet perpendicular to the plane of the figure there are more electrons flowing to the left than to the right because of the density gradient.

so that plasma oscillations do not occur we may include a time-dependent electric field as we shall see in Section 2.12.

2.6 Time-varying magnetic field and adiabatic invariance

In Section 2.4 we introduced certain inhomogeneous magnetic fields. In practice, one often has to deal with fields that are time-dependent. In keeping with Section 2.4, which was restricted to weakly inhomogeneous fields, we shall consider only magnetic fields varying slowly in time ($|\dot{\mathbf{B}}|/|\mathbf{B}| \ll |\Omega|$). For simplicity, consider a magnetic field which varies in time but not in space. For particle motion in such a field, can one find conserved quantities that are counterparts to $W_\perp$, $W_\parallel$ for motion in a constant and uniform magnetic field? We shall demonstrate that such invariants do exist in particular circumstances.

A time-dependent axial magnetic field induces an azimuthal electric field, $\mathbf{E}$, so that, unlike $v_\parallel$, $v_\perp$ is no longer constant and taking the scalar product of (2.1) with $v_\perp$ gives

$$\frac{\mathrm{d}}{\mathrm{d}t}\left(\tfrac{1}{2}mv_\perp^2\right) = e\mathbf{E}\cdot\mathbf{v}_\perp$$

Thus in executing a Larmor orbit the particle energy changes by

$$\delta\left(\tfrac{1}{2}mv_\perp^2\right) = \oint \mathbf{E}\cdot\mathrm{d}\mathbf{r}_\perp = e\int(\boldsymbol{\nabla}\times\mathbf{E})\cdot\mathrm{d}\mathbf{S}$$

where $\mathrm{d}\mathbf{r}_\perp = \mathbf{v}_\perp\,\mathrm{d}t$ and $\mathrm{d}\mathbf{S}$ is an element of the surface enclosed by the orbital path. Hence, from (2.2)

$$\delta\left(\tfrac{1}{2}mv_\perp^2\right) = -e\int\frac{\partial\mathbf{B}}{\partial t}\cdot\mathrm{d}\mathbf{S}$$

Since the field changes slowly

$$\delta\left(\tfrac{1}{2}mv_\perp^2\right) \simeq \pi {r_L}^2 |e|\dot{B} = \frac{mv_\perp^2}{2}\frac{2\pi}{|\Omega|}\frac{\dot{B}}{B}$$

Note in passing that the negative sign disappears since for positive (negative) charges $e > 0$ (< 0) and $\mathbf{B} \cdot \mathrm{d}\mathbf{S} < 0$ (> 0). If we denote by δB the change in magnitude of the magnetic field during one orbit it follows that

$$\delta W_\perp = W_\perp \frac{\delta B}{B}$$

i.e.

$$\delta(W_\perp / B) = 0$$

From Section 2.2.1 where we identified the magnetic moment of a charged particle as

$$\mu_\mathrm{B} = \frac{W_\perp}{B} \tag{2.29}$$

we see from this analysis that μ_B is an approximate constant of the motion, a property first recognized by Alfvén.

The magnetic moment is one of a number of entities which are approximate constants of the motion for particles in magnetic fields. In Hamiltonian dynamics such quantities are known as *adiabatic invariants*. In particular the *action* $\oint p\,\mathrm{d}q$, where p, q are conjugate canonical variables and the integral is taken over a period of the motion in q, is adiabatically invariant. The condition critical for adiabatic invariance is that the particle trajectory changes *slowly* on the time scale of the basic periodic motion. The number of invariants is determined by the periodicities that characterize the motion. We have established that the adiabatic invariance of μ_B is associated with Larmor precession in a magnetic field. We shall find that a charged particle may be trapped between magnetic mirror fields, as a result of which another periodicity appears and with it a second adiabatic invariant. If in addition we allow for curvature drift then for a suitably configured field a third invariant may be identified corresponding to the magnetic flux enclosed by the drift orbit of the guiding centre.

2.6.1 Invariance of the magnetic moment in an inhomogeneous field

The magnetic moment also turns out to be invariant for motion in spatially inhomogeneous magnetic fields for which the matrix $[\partial B_i / \partial x_j]$ has non-zero diagonal elements, the divergence terms. To demonstrate this, consider the axially symmetric magnetic field increasing slowly with z as in Fig. 2.6. Writing the divergence

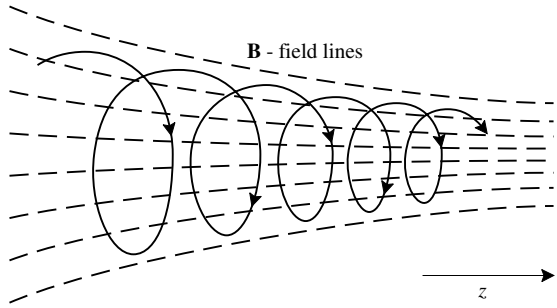

Fig. 2.6. Magnetic field increasing in the direction of the field.

property of **B** in cylindrical polar coordinates and integrating gives

$$r B_r = -\int_0^r r \frac{\partial B_z}{\partial z}\,\mathrm{d}r$$

Since the field is approximately constant over one Larmor orbit and $|B_r| \ll B_z$

$$B_r(r_\mathrm{L}) \simeq -\frac{r_\mathrm{L}}{2}\frac{\partial B_z}{\partial z} \simeq -\frac{r_\mathrm{L}}{2}\frac{\partial B}{\partial z}$$

With this approximation the z component of (2.1) gives

$$m\frac{\mathrm{d}v_\parallel}{\mathrm{d}t} = -\tfrac{1}{2}|e|r_\mathrm{L}v_\perp\frac{\partial B}{\partial z} = -\frac{W_\perp}{B}\frac{\partial B}{\partial z} = -\mu_\mathrm{B}\frac{\partial B}{\partial z}$$

Thus,

$$\frac{\mathrm{d}}{\mathrm{d}t}\left(\tfrac{1}{2}m{v_\parallel}^2\right) = -\mu_\mathrm{B}v_\parallel\frac{\partial B}{\partial z} = -\mu_\mathrm{B}\frac{\mathrm{d}B}{\mathrm{d}t} \tag{2.30}$$

From (2.29)

$$\frac{\mathrm{d}}{\mathrm{d}t}\left(\tfrac{1}{2}m{v_\perp}^2\right) \equiv \frac{\mathrm{d}}{\mathrm{d}t}(\mu_\mathrm{B}B) \tag{2.31}$$

Adding (2.30) and (2.31) and using energy conservation we find

$$\frac{\mathrm{d}\mu_\mathrm{B}}{\mathrm{d}t} = 0 \tag{2.32}$$

The invariance of μ_B in spatially varying magnetic fields has important implications which we explore in the next section.

2.7 Magnetic mirrors

Consider a particle moving in the inhomogeneous field introduced in Section 2.6 towards the region of increasing B. It follows from the invariance of $W_\perp/B$ that

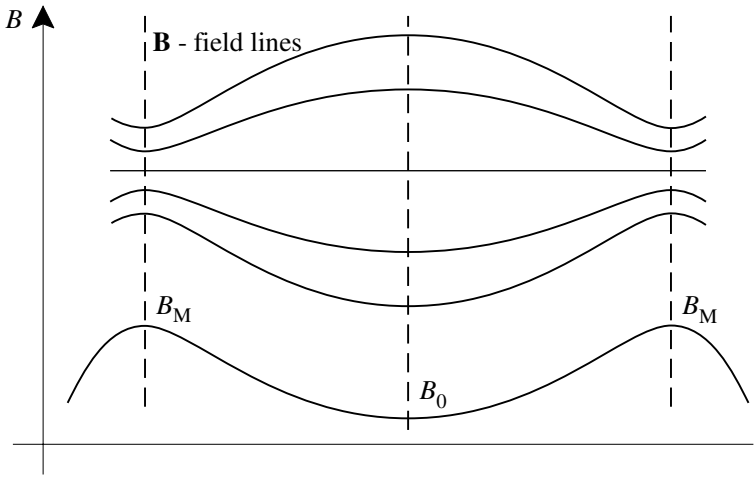

Fig. 2.7. Magnetic mirror field.

$W_\perp$ must increase. Since energy is conserved this increase must be at the expense of $W_\parallel$. Thus it may happen that for some value of B (B_R say) $W_\parallel = 0$, in which case the particle cannot penetrate further into the magnetic field and suffers reflection at this point (provided $(\mathbf{v} \times \mathbf{B}) \cdot \hat{\mathbf{z}} \neq 0$). Such a field configuration has the properties of a *magnetic mirror*.

It is convenient to define the *pitch angle*, θ, of the particle by

$$\tan\theta = \frac{v_\perp}{v_\parallel} \tag{2.33}$$

Then, from the invariance of $\mu_B = W_\perp/B$, it follows that $\sin^2\theta/B$ is constant. Defining the constant by B_R^{-1} we have

$$\sin\theta = (B/B_R)^{1/2} \tag{2.34}$$

For a particle which penetrates to the point where B reaches its maximum value B_M before being reflected, $B_R = B_M$. Hence particles with pitch angles such that $\sin\theta > (B/B_M)^{1/2}$ suffer reflection before reaching the region of maximum field; those having $\sin\theta \leq (B/B_M)^{1/2}$ are not reflected.

If one arranges two mirror fields in the configuration shown in Fig. 2.7 then particles with $\sin\theta > (B/B_M)^{1/2}$ will be reflected to and fro. This configuration constitutes a *magnetic bottle* or *adiabatic mirror trap*. Taking B_0 to be the value of the magnetic field in the mid-plane of the bottle, the *mirror ratio* is defined by

$$R = \frac{B_M}{B_0}$$

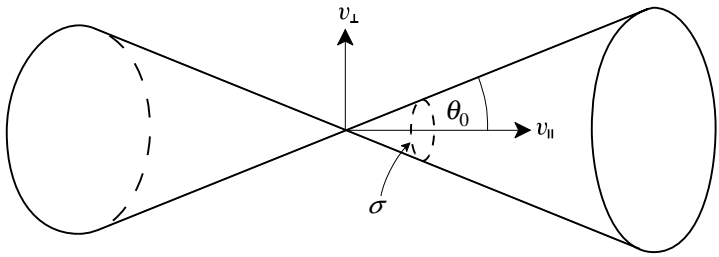

Fig. 2.8. Loss cone for a magnetic mirror. Particles with velocities within the cone will escape from the mirror.

and particles will be reflected if

$$\sin\theta_0 > R^{-1/2}$$

The particles which are lost from the magnetic bottle are those within the solid angle σ in velocity space shown in Fig. 2.8. This solid angle σ defines the *loss cone*. Denoting the probability of loss from the bottle by P where

$$P = \frac{\sigma}{2\pi} = \int_0^{\theta_0} \sin\theta \, \mathrm{d}\theta$$

we have

$$P = 1 - \left(\frac{R-1}{R}\right)^{1/2} \simeq \frac{1}{2R} \qquad \text{if } R \gg 1$$

Thus the higher the mirror ratio, the less likely it is that particles will escape.

Mirror traps have been used to contain laboratory plasmas but losses through the mirrors led to their being abandoned in favour of toroidal devices. However, the concept of magnetic trapping is fundamental to an understanding of many naturally occurring plasmas such as the Earth's radiation belts and the energetic particles associated with solar flares which move in closed loop fields associated with active regions of the Sun. Before discussing naturally occurring magnetic traps we first identify a second adiabatic invariant.

2.8 The longitudinal adiabatic invariant

Given that the number of adiabatic invariants reflects the distinct system periodicities, we expect a second invariant to arise in connection with the reflection of particles between the fields of a mirror trap. This invariant is associated with the guiding centre motion and is known as the *longitudinal invariant*, J, defined by

$$J = \oint v_\parallel \, \mathrm{d}s \tag{2.35}$$

where ds is an element of the guiding centre path and the integral is evaluated over one complete traverse of the guiding centre. The invariance of J is useful in situations in which the mirror points are no longer stationary; therefore B is taken to be slowly varying in both space and time. Since J is a function of $\dot{s}$ ($\equiv v_\parallel$), s, t, using $W = \frac{1}{2}mv_\parallel^2 + \mu_\mathrm{B}B$ we may write

$$J(W, s, t) = \int_{s_1}^{s} \left[\frac{2}{m}(W - \mu_\mathrm{B}B)\right]^{1/2} \mathrm{d}s \tag{2.36}$$

Then

$$\begin{aligned}
\frac{\mathrm{d}J}{\mathrm{d}t} &= \left(\frac{\partial J}{\partial t}\right)_{W,s} + \left(\frac{\partial J}{\partial W}\right)_{s,t}\frac{\mathrm{d}W}{\mathrm{d}t} + \left(\frac{\partial J}{\partial s}\right)_{W,t}\frac{\mathrm{d}s}{\mathrm{d}t} \\
&= -\int_{s_1}^{s}\left[\frac{2}{m}(W - \mu_\mathrm{B}B)\right]^{-1/2}\left(\frac{\mu_\mathrm{B}}{m}\frac{\partial B}{\partial t}\right)\mathrm{d}s \\
&\quad + \left\{v_\parallel\dot{v}_\parallel + \frac{\mu_\mathrm{B}}{m}\frac{\partial B}{\partial t} + \frac{\mu_\mathrm{B}}{m}v_\parallel\frac{\partial B}{\partial s}\right\}\int_{s_1}^{s}\left[\frac{2}{m}(W - \mu_\mathrm{B}B)\right]^{-1/2}\mathrm{d}s \\
&\quad + \left[\frac{2}{m}(W - \mu_\mathrm{B}B)\right]^{1/2}v_\parallel - v_\parallel\int_{s_1}^{s}\left[\frac{2}{m}(W - \mu_\mathrm{B}B)\right]^{-1/2}\left(\frac{\mu_\mathrm{B}}{m}\frac{\partial B}{\partial s}\right)\mathrm{d}s
\end{aligned}$$

Now, at the turning point $s = s_1$, $v_\parallel = 0$; then

$$\begin{aligned}
\frac{\mathrm{d}J(W, s_1, t)}{\mathrm{d}t} &= -\oint\left[\frac{2}{m}(W - \mu_\mathrm{B}B)\right]^{-1/2}\left(\frac{\mu_\mathrm{B}}{m}\frac{\partial B}{\partial t}\right)\mathrm{d}s \\
&\quad + \frac{\mu_\mathrm{B}}{m}\frac{\partial B}{\partial t}\oint\left[\frac{2}{m}(W - \mu_\mathrm{B}B)\right]^{-1/2}\mathrm{d}s \\
&= -\oint\left(\frac{\mu_\mathrm{B}}{m}\frac{\partial B}{\partial t}\right)\frac{\mathrm{d}s}{v_\parallel} + \frac{\mu_\mathrm{B}}{m}\frac{\partial B}{\partial t}\oint\frac{\mathrm{d}s}{v_\parallel} \\
&= -\int_0^{\tau_\parallel}\frac{\mu_\mathrm{B}}{m}\frac{\partial B}{\partial t}\,\mathrm{d}t + \frac{\mu_\mathrm{B}}{m}\frac{\partial B}{\partial t}\int_0^{\tau_\parallel}\mathrm{d}t \\
&= -\frac{\mu_\mathrm{B}}{m}\left[B(\tau_\parallel) - B(0) - \tau_\parallel\frac{\partial B}{\partial t}\right] \\
&\sim O(\tau_\parallel/t_\mathrm{F})^2
\end{aligned}$$

where $\tau_\parallel$ is the transit time and t_F the time scale for changes in B. Provided $t_\mathrm{F} \gg \tau_\parallel$

$$\frac{\mathrm{d}J}{\mathrm{d}t} = 0 \tag{2.37}$$

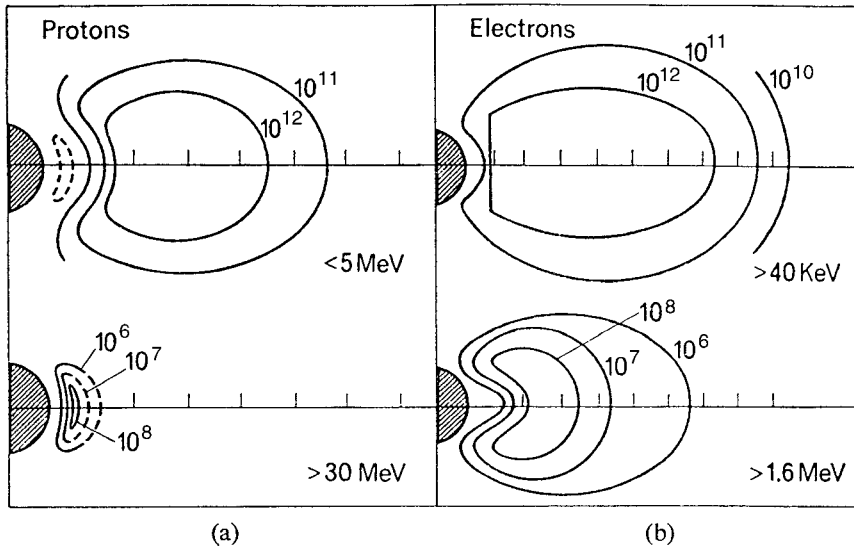

Fig. 2.9. Earth's radiation belts showing schematic spatial distributions of trapped protons (a) and electrons (b) across the energy ranges indicated. The contour label is the flux of charged particles in units (number $m^{-2}\,s^{-1}$).

Thus J is an adiabatic invariant. Since the transit time between mirror points is many Larmor periods, the condition on $\partial B/\partial t$ in order that J be invariant is clearly more stringent than that for μ_B. One can establish the adiabatic invariance of J more generally by including a slowly varying time-dependent electric field. A relativistic proof of J-invariance was given by Northrop and Teller (1960).

2.8.1 Mirror traps

Invariance of J is a particularly useful concept in determining particle trajectories in complex magnetic fields and is often used in practice in preference to integrating the guiding centre equations. One such application serves to characterize particles injected into, and trapped by, the geomagnetic field. Van Allen and co-workers first identified regions of energetic particles encircling the Earth in 1958. These structures are known as the *Van Allen radiation belts* and similar belts have since been identified in other planets where magnetospheres are present. The morphology of the Earth's radiation belts is complex, consisting of two regions, an inner and an outer belt, shown schematically in Fig. 2.9. Protons of energies from 30 to a few hundred MeV were observed extending out to about $2R_E$, where R_E is the Earth radius. Protons populating the outer belt are much less energetic. There is no comparable demarcation in the electron energy distribution across the two

regions represented in Fig. 2.9. The distribution of electrons in the outer radiation belt stretches virtually as far as the magnetopause at $\sim 10R_{\mathrm{E}}$.

The particle populations in the Van Allen belts are distinct from ionospheric distributions on the one hand and those of the solar wind on the other. Identifying the sources of the Van Allen populations provides a key to understanding the morphology of the radiation belts. The inner belt is characterized not only by its energy distribution but by the fact that it is more stable than the outer belts. Taken together these observations suggest distinct sources for inner and outer belt components. Cosmic rays colliding with atoms result in disintegrations into nuclear components. These include neutrons travelling outwards which decay to produce energetic protons and electrons. Observations have confirmed that cosmic rays are indeed a source for inner belt protons with energies of tens of MeV. The low energy component on the other hand is thought to derive from an ionospheric source while those at intermediate energies are variously solar wind particles that have been accelerated as well as particles injected from the plasma sheet during auroral events.

Although the detailed dynamics of the radiation belts is complicated it is clear that the geomagnetic field serves as a magnetic trap for charged particles. The geomagnetic field may be represented as a dipole (at any rate out to distances of about $5R_{\mathrm{E}}$ beyond which the field is distorted by the solar wind) with the field lines bunching at the north and south poles. Energetic particles injected into the Earth's magnetic field will describe helical trajectories and undergo reflection in the stronger field regions around the magnetic poles, transit times for protons bouncing between mirror points being of the order of a second. The stability of the Van Allen belts is essentially a reflection of the invariance of J.

In addition to the bounce motion between mirror points, the results of Section 2.4 mean that particles drift azimuthally since field lines are curved and there exists a magnetic field gradient normal to the direction of $\mathbf{B}$. Electrons drift from west to east and protons vice versa. For an electron with energy 40 keV, the time taken for the guiding centre to complete a circuit is of the order of an hour. The guiding centre of a particle generates a surface of rotation, which in some circumstances may be closed. The periodicity associated with this drift leads to a third adiabatic invariant in magnetic fields with suitable morphology.

2.9 Magnetic flux as an adiabatic invariant

The third adiabatic invariant is the flux Φ of the magnetic field through the surface of rotation. A formal proof of the adiabatic invariance of Φ was given by Northrop (1961). We present here a précis of Northrop's proof. It is convenient to use a set of curvilinear coordinates (α, β, s) where $\alpha(\mathbf{r}, t)$, $\beta(\mathbf{r}, t)$ are parameters character-

izing a field line and therefore constant on it while s represents distance along the line. The parameters α and β, known as *Clebsch variables*, are chosen so that

$$\mathbf{A} = \alpha \nabla \beta \qquad \mathbf{B} = \nabla \alpha \times \nabla \beta \tag{2.38}$$

where $\mathbf{A}$ is the magnetic vector potential.

For time-dependent magnetic fields the particle energy $K = \frac{1}{2} m v_\parallel^2 + \mu_B B + e\alpha \partial\beta/\partial t$ is no longer a constant of motion. The flux Φ through the longitudinal invariant surface is a function of J, μ_B, K and t but since the first pair are known adiabatic invariants we suppress this dependence and represent the flux as $\Phi(K, t)$. Then

$$\Phi(K, t) = \oint \mathbf{A} \cdot \mathrm{d}\mathbf{l} = \oint \alpha \nabla \beta \cdot \mathrm{d}\mathbf{l} = \oint \alpha \, \mathrm{d}\beta$$

in which the contour is any simply connected curve lying on the surface and

$$\frac{\mathrm{d}\Phi}{\mathrm{d}t} = \frac{\partial \Phi(K, t)}{\partial K} \langle \dot{K} \rangle_\parallel + \frac{\partial \Phi(K, t)}{\partial t} \tag{2.39}$$

where $\langle \dot{K} \rangle_\parallel$ indicating an average of $\dot{K}$ over motion along the field lines has been substituted for $\dot{K}$ since changes over a longitudinal transit time are not of interest here. It is straightforward to show that (see Exercise 2.4)

$$\frac{\partial \Phi}{\partial K} = \oint \frac{\partial \alpha}{\partial K} \mathrm{d}\beta = \frac{1}{e} \oint \frac{\mathrm{d}\beta}{\langle \dot{\beta} \rangle} = \frac{\tau_P}{e}$$

$$\frac{\partial \Phi}{\partial t} = \oint \frac{\partial \alpha}{\partial t} \mathrm{d}\beta = -\frac{1}{e} \oint \frac{\langle \dot{K} \rangle_\parallel \mathrm{d}\beta}{\langle \dot{\beta} \rangle} = -\frac{\tau_P}{e} \langle \langle \dot{K} \rangle_\parallel \rangle_P$$

where τ_P denotes the period of precession of the guiding centre and $\langle \langle \dot{K} \rangle_\parallel \rangle_P$ is the average of $\langle \dot{K} \rangle_\parallel$ over a precession period. From these relations we see that

$$\frac{\mathrm{d}\Phi}{\mathrm{d}t} = \frac{\tau_P}{e} \left[\langle \dot{K} \rangle_\parallel - \langle \langle \dot{K} \rangle_\parallel \rangle_P \right] \tag{2.40}$$

Although $\mathrm{d}\Phi/\mathrm{d}t \neq 0$ it is evident that the average rate of change of the magnetic flux over a period of precession does vanish, i.e.

$$\left\langle \frac{\mathrm{d}\Phi}{\mathrm{d}t} \right\rangle_P = 0 \tag{2.41}$$

Hence although K is no longer invariant for time-dependent magnetic fields, a new adiabatic invariant Φ has been found in its place. A fuller discussion of the properties of invariant surfaces has been given by Northrop (1963).

A summary of the properties of the three adiabatic invariants μ_B, J, and Φ is set out in Table 2.1. It is perhaps worth noting that the stringent requirements demanded of Φ (associated with the loss of phase information in averaging over closed trajectories) make it a less useful invariant in practice than either μ_B or J.

Table 2.1. *Adiabatic invariants*

Invariant	Particle characteristic motion	Periodicity	Validity conditions
Magnetic moment $\mu_B = W_\perp/B$	Larmor orbit	$\tau_L = 2\pi/\lvert\Omega\rvert$ $v_\perp^2 \tau_L \simeq$ const.	$\tau_L \ll t_F$
Longitudinal invariant $J = \oint v_\parallel \, ds$	Longitudinal bounce between mirror fields	$\tau_\parallel$ $\langle v_\parallel^2 \rangle \tau_\parallel \simeq$ const.	$\tau_L \ll \tau_\parallel \ll t_F$ μ_B constant
Flux invariant $\Phi = \int \mathbf{B} \cdot d\mathbf{S}$	Azimuthal precession; drift velocity, v_p	τ_P $\langle v_P^2 \rangle \tau_P \simeq$ const.	$\tau_L \ll \tau_\parallel \ll \tau_P \ll t_F$ μ_B constant J constant

2.10 Particle orbits in tokamaks

Electron trapping in spatially inhomogeneous magnetic fields is important in the physics of tokamaks. In Chapter 1 we saw that a tokamak is characterized by a combination of toroidal and poloidal magnetic fields, B_t and B_p respectively, since a toroidal field on its own is not capable of containing a plasma in equilibrium. Anticipating our discussion of toroidal equilibria in Chapter 4, tokamaks are characterized by an ordering of these fields such that $B_t \gg B_p$. The magnetic field lines are helices wound on a toroidal surface. Particles whose guiding centres follow such helical field lines and whose velocity components along the field are high enough that they cycle round the torus make up the population of *passing* particles. In contrast particles with lower velocities parallel to the field contribute to the population of particles trapped on the outer side of the torus between magnetic mirrors created by the poloidal variation of the field. The tokamak magnetic field varies as $1/R$ where $R = R_0 + r\cos\theta$; R_0 is the major radius of the tokamak and r the minor radius of the surface on which the guiding centre of the particle lies, with θ the poloidal angle. The ratio $r/R_0 = \epsilon$ is known as the *inverse aspect ratio* and serves as an expansion parameter. The magnetic field $B(\theta)$ may then be expressed as

$$B(\theta) = B(0)(1 - \epsilon\cos\theta)/(1 - \epsilon) \tag{2.42}$$

From the adiabatic invariance of μ_B we find

$$\frac{v_\parallel^2}{v_0^2} = 1 - \frac{v_{\perp 0}^2}{v_0^2}\left(\frac{1-\epsilon\cos\theta}{1-\epsilon}\right)$$

It is clear from this expression that $v_\parallel$ will vanish for θ satisfying

$$\frac{v_{\parallel 0}^2}{v_{\perp 0}^2} = \epsilon(1-\cos\theta) \tag{2.43}$$

where the right-hand side can assume values up to 2ϵ (at $\theta = \pi$). Clearly if $v_{\parallel 0}^2/v_{\perp 0}^2 > 2\epsilon$, (2.43) cannot be satisfied and this condition defines the population of *passing* particles. On the other hand if $v_{\parallel 0}^2/v_{\perp 0}^2 < 2\epsilon$ there will be some value of θ given by (2.43) for which $v_\parallel = 0$. This condition serves to define the population of *trapped* particles.

Consider in turn the characteristics of passing and trapped particles. Two effects contribute to the dynamics of passing particles. Superposed on the motion parallel to the magnetic field which gives rise to rotation in the poloidal direction with velocity $\mathbf{v}_p = (\mathbf{B}_p/B_t)v_\parallel$ is a combination of gradient and curvature drifts in the toroidal magnetic field. Given that B_t is approximately inversely proportional to the major radius R, it follows that the drift velocity $\mathbf{v}_B$ defined by (2.24) is in the vertical direction, $\hat{\mathbf{z}}$. If we suppose that the cross-section is approximately circular, the motion of the guiding centre projected on to the poloidal plane may be represented as

$$\frac{\dot{r}}{r\dot{\theta}} = \frac{v_B\sin\theta}{v_p + v_B\cos\theta} \tag{2.44}$$

The drift orbit is thus

$$\frac{r}{r_0} = \left[1 + \frac{v_B}{v_p}\cos\theta\right]^{-1} \tag{2.45}$$

where $r = r_0$ for $\theta = \pi/2$. The displacement of this distorted circle in the direction of the major radius is determined by

$$|\Delta_{pass}| = r_0\left(\frac{v_B}{v_\parallel}\right)\left(\frac{B_t}{B_p}\right) = \frac{q}{\Omega}\frac{(v_\parallel^2 + \frac{1}{2}v_\perp^2)}{v_\parallel} \sim \left(\frac{v_\parallel^2 + \frac{1}{2}v_\perp^2}{v_\perp v_\parallel}\right) q r_L \tag{2.46}$$

where $q = r_0 B_t/RB_p$ is a quantity known as the *safety factor* (see Section 4.3.1) and r_L is the particle Larmor radius in the toroidal magnetic field. For tokamaks, q is typically about 3 near the plasma edge so that for passing particles the shift of the drift orbit, shown in Fig. 2.10, is significantly bigger than a Larmor radius.

Dealing with the trapped particles is more difficult but by making use of constants of the motion one can determine the size of the drift orbits for this population

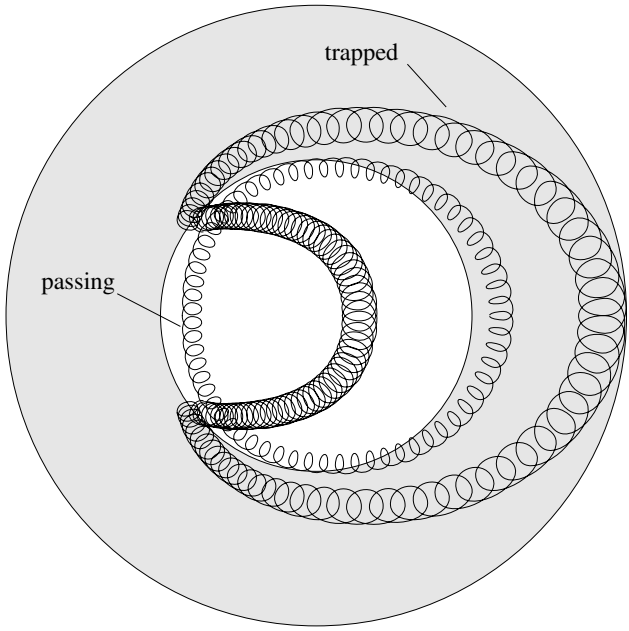

Fig. 2.10. Orbits of passing and trapped particles in a tokamak projected on the poloidal plane.

as well. The procedure is outlined in Exercise 2.5. Trapped particles describe the *banana* orbits shown in Fig. 2.10. The width of a banana orbit is approximately

$$|\Delta_{\mathrm{tr}}| \sim 2\left(\frac{2R}{r}\right)^{\frac{1}{2}} q r_{\mathrm{L}} \tag{2.47}$$

We see from this estimate that trapped particle orbits can be an order of magnitude bigger than a Larmor radius.

2.11 Adiabatic invariance and particle acceleration

Particle acceleration is of widespread interest in both laboratory and space plasmas. As an example we consider an idea originally put forward by Fermi (1949) to account for the very energetic particles ($O(10^{18}\,\mathrm{eV})$) in cosmic radiation. How such enormous energies are attained is obviously a key question in cosmic ray theory. Fermi postulated that there are regions of space in which clumps of magnetic field of higher than average intensity occur with charged particles trapped between them. He argued that these magnetic clumps would not be static and trapped particles could be accelerated if such regions were approaching one another. By the same token, particles would lose energy in mirror regions that were separating. Fermi

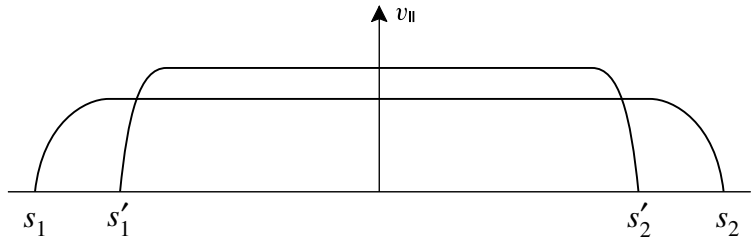

Fig. 2.11. Variation of $v_\parallel$ between mirror points s_1 and s_2. If the field maxima approach one another, so do the mirror points and at some later time the phase trajectory is given by the curve from s_1' to s_2'.

showed that the probability of head-on collisions was greater than that of overtaking collisions, their relative frequencies being proportional to $(v_\parallel + v_B)/(v_\parallel - v_B)$ where v_B is the velocity of the magnetic clump.

To see how Fermi acceleration works suppose a charged cosmic ray particle is trapped between two magnetic mirrors which move towards one another sufficiently slowly that J is a good adiabatic invariant. Suppose too that at $t = 0$ the coordinates of the mirror points in the phase space diagram, Fig. 2.11, are s_1 and s_2, while at some later time, t', they shift to s_1' and s_2' respectively. The invariance of J means that the area enclosed by the phase space orbit is constant. Denoting $s_1 - s_2$ by s_0, $s_1' - s_2'$ by s_0' gives

$$v_\parallel' \simeq v_\parallel \frac{s_0}{s_0'}$$

where $v_\parallel$, $v_\parallel'$ are the parallel components of velocity at the mid-plane at $t = 0$, $t = t'$, respectively. Then

$$W_\parallel' = \left(\frac{s_0}{s_0'}\right)^2 W_\parallel$$

and

$$W' = W_\perp' + W_\parallel' = \frac{m}{2}\left[v_\perp^2 + \left(\frac{s_0}{s_0'}\right)^2 v_\parallel^2\right]$$

by making use of the invariance of μ_B (assuming the field is constant at the mid-plane). Thus the energy of a particle trapped between slowly approaching magnetic mirrors increases. As proposed originally, Fermi acceleration suffers from a serious limitation. For increasing $v_\parallel$, the pitch angle defined by (2.33) decreases so that at some stage a particle being accelerated falls into the loss cone and escapes, thus limiting the gain in energy.

2.12 Polarization drift

Up to this point we have not allowed for any time-dependent electric fields, having set $\dot{E} = 0$ (in Section 2.5) to exclude plasma oscillations. We now want to relax this condition and allow for a *slow* time variation in an applied electric field. Doing so introduces yet another drift, the *polarization drift*, to add to those discussed earlier. To see how polarization drift comes about, we return to the configuration analysed in Section 2.3 with an electric field acting in a direction perpendicular to an applied magnetic field. By slow time dependence of the electric field we mean slow compared with the Larmor period of the particle. Starting with (2.12) and (2.13) which we used to identify the $\mathbf{E} \times \mathbf{B}$ drift, we introduce a transformation $\dot{X} = \dot{x} - eE_\perp/m\Omega$ to move to the drift frame. In this frame

$$\ddot{X} = \Omega\left(\dot{y} - \frac{e}{m\Omega^2}\frac{\mathrm{d}E_\perp}{\mathrm{d}t}\right) \qquad \ddot{y} = -\Omega\dot{X} \tag{2.48}$$

If we now apply a second transformation

$$\dot{Y} = \dot{y} - \frac{e}{m\Omega^2}\frac{\mathrm{d}E_\perp}{\mathrm{d}t}$$

and make use of the fact that the time scale of variation of the electric field is much longer than a Larmor period, the equations of motion in this new frame reduce to the Larmor equations for motion in a magnetic field alone. This establishes that in addition to the $\mathbf{E} \times \mathbf{B}$ drift there is now a polarization drift, with drift velocity $\mathbf{v}_\mathrm{P}$ given by

$$\mathbf{v}_\mathrm{P} = \frac{m}{eB^2}\frac{\mathrm{d}\mathbf{E}}{\mathrm{d}t} \tag{2.49}$$

The polarization drift has distinct properties compared with the $\mathbf{E} \times \mathbf{B}$ drift. Since $\mathbf{v}_\mathrm{P}$ is charge-dependent, electron and ion drifts are in opposite directions but the mass dependence means that the ion drift is dominant. Associated with the drift is a *polarization current density*

$$\mathbf{j}_\mathrm{p} \simeq \frac{n_\mathrm{i} m_\mathrm{i}}{B^2}\frac{\mathrm{d}\mathbf{E}}{\mathrm{d}t}$$

which contributes to the total current density in general (see Section 2.5). The name polarization drift comes from the fact that the electric field inside most plasmas derives not from an externally applied source but from the polarization of the plasma due to charge separation.

2.13 Particle motion at relativistic energies

To describe the motion of particles of relativistic energy we have to revert to the full Lorentz equation,

$$\frac{\mathrm{d}}{\mathrm{dt}}(\gamma m\mathbf{v}) = e(\mathbf{E} + \mathbf{v} \times \mathbf{B}) \tag{2.50}$$

where $\gamma = (1-v^2/c^2)^{1/2}$. It is possible to set about solving the Lorentz equation for the various field configurations considered earlier. For example a particle moving with relativistic velocity in a constant, uniform magnetic field $\mathbf{B}$, with energy $\mathcal{E} = \gamma mc^2$ is now characterized by a Larmor frequency

$$\Omega = \frac{eB}{m\gamma} \tag{2.51}$$

In the case of motion in constant, uniform electric and magnetic fields we no longer need to insist that $E_\parallel = 0$ as in Section 2.3. In general one can repeat the analysis of slowly varying magnetic fields in the drift approximation using the full Lorentz equation and again establish the existence of adiabatic invariants. However, these exercises are of limited value and rather than go down this road we turn instead to a problem of greater practical interest, the relativistic motion of particles in an electromagnetic field.

2.13.1 Motion in a monochromatic plane-polarized electromagnetic wave

For a plane-polarized wave propagating in the x direction, $\mathbf{E} = (0, E, 0)$, and $\mathbf{B} = (0, 0, B)$. We can conveniently describe the fields by their vector potential, $\mathbf{A} = (0, a(\tau)\cos\omega\tau, 0)$, where a is the amplitude of the wave, ω the frequency, and $\tau = t - x/c$. For a truly monochromatic wave a is constant. In practice, however, a can never be constant since the amplitude must grow from zero when the wave is switched on. Moreover, treatments which assume a is constant lead to solutions depending critically on the initial phase and thereby predict electron drifts in arbitrary directions (see Exercise 2.7). For an almost monochromatic wave, $a(\tau)$ must be a slowly varying function and the only significant effect of including its variation is to ensure that the fields are initially zero; dependence on the initial phase does not then appear. $\mathbf{E}$ and $\mathbf{B}$ are given by the usual equations

$$\mathbf{E} = -\frac{\partial \mathbf{A}}{\partial t} \qquad \mathbf{B} = \boldsymbol{\nabla} \times \mathbf{A}$$

from which it follows in the case of a plane-polarized wave

$$E = cB = -\frac{\mathrm{d}A}{\mathrm{d}\tau}$$

The relativistic Lorentz equation gives

$$\frac{\mathrm{d}}{\mathrm{d}t}(\gamma\dot{x}) = \frac{eB}{m}\dot{y} = -\frac{e}{mc}\dot{y}\frac{\mathrm{d}A}{\mathrm{d}\tau} \tag{2.52}$$

$$\frac{\mathrm{d}}{\mathrm{d}t}(\gamma\dot{y}) = \frac{e}{m}(E - B\dot{x}) = -\frac{e}{mc}(c - \dot{x})\frac{\mathrm{d}A}{\mathrm{d}\tau} \tag{2.53}$$

$$\frac{\mathrm{d}}{\mathrm{d}t}(\gamma\dot{z}) = 0 \tag{2.54}$$

$$\frac{\mathrm{d}}{\mathrm{d}t}(\gamma c) = \frac{eE}{mc}\dot{y} = -\frac{e}{mc}\dot{y}\frac{\mathrm{d}A}{\mathrm{d}\tau} \tag{2.55}$$

Subtracting (2.52) from (2.55) gives, on integrating,

$$1 - \dot{x}/c = (1 - v^2/c^2)^{1/2} \tag{2.56}$$

assuming that the electron is initially at rest at the origin. Since

$$\frac{\mathrm{d}\tau}{\mathrm{d}t} = 1 - \frac{\dot{x}}{c} \tag{2.57}$$

(2.53) may be integrated directly:

$$\frac{\dot{y}/c}{(1 - v^2/c^2)^{1/2}} = -\frac{eA}{mc} \tag{2.58}$$

Substituting for $\dot{y}$ from (2.58) and using (2.56) and (2.57), (2.52) becomes

$$\frac{\mathrm{d}}{\mathrm{d}t}(\gamma\dot{x}/c) = \left(\frac{e}{mc}\right)^2 A\frac{\mathrm{d}A}{\mathrm{d}\tau}\frac{\mathrm{d}\tau}{\mathrm{d}t}$$

Hence,

$$\gamma\dot{x}/c = \frac{1}{2}\left(\frac{eA}{mc}\right)^2$$

Finally, using (2.56) and (2.57) again,

$$\dot{x} = \frac{c}{2}\left(\frac{eA}{mc}\right)^2\frac{\mathrm{d}\tau}{\mathrm{d}t} = \frac{c}{2}a_0^2\frac{\mathrm{d}\tau}{\mathrm{d}t}\cos^2\omega\tau \tag{2.59}$$

$$\dot{y} = -c\left(\frac{eA}{mc}\right)\frac{\mathrm{d}\tau}{\mathrm{d}t} = -ca_0\frac{\mathrm{d}\tau}{\mathrm{d}t}\cos\omega\tau \tag{2.60}$$

and from (2.54)

$$\dot{z} = 0 \tag{2.61}$$

where $a_0 = (ea/mc)$. Averaging $\dot{x}$ over one period ($T = 2\pi/\omega$), $a(\tau)$ may be treated as constant,

$$\langle \dot{x} \rangle = \frac{\int \dot{x}\, \mathrm{d}t}{\int \mathrm{d}t} = \frac{\frac{c}{2}a_0^2 \int \cos^2 \omega\tau \, \mathrm{d}\tau}{\int (\mathrm{d}\tau + \mathrm{d}x/c)}$$

$$= \frac{\frac{c}{2}a_0^2 \int \cos^2 \omega\tau \, \mathrm{d}\tau}{\int \mathrm{d}\tau \left(1 + \frac{1}{2}a_0^2 \cos^2 \omega\tau\right)} = \frac{ca_0^2}{4 + a_0^2} \tag{2.62}$$

Similarly,

$$\langle \dot{y} \rangle = 0$$

For $a_0 < 1$, the motion is effectively the quiver motion of the electron in the **E** field of the wave (i.e. along Oy) but in addition the electron drifts in the direction of propagation of the wave with drift velocity

$$\mathbf{v}_{\mathrm{W}} = \frac{e^2}{2m^2\omega^2} \langle \mathbf{E} \times \mathbf{B} \rangle \tag{2.63}$$

For highly relativistic electrons $a_0 \gg 1$ and $\langle \dot{x} \rangle \to c$. Electrons with relativistic energies appear as a consequence of the interaction of ultra-intense laser light (typically $\sim 10^{20}\,\mathrm{W\,cm^{-2}}$) with plasmas. Evidence of electrons drifting in the direction of propagation of the light has been found from both simulations and experiments. An interesting effect of this drift velocity is to predict a Doppler shift in the frequency of light scattered by free electrons (see Kibble (1964)).

It is a straightforward exercise to integrate the equations of motion to determine the electron trajectory, which has the form of a figure-of-eight. Experiments by Chen, Maksimchuk and Umstadter (1998) have confirmed the figure-of-eight trajectory.

2.14 The ponderomotive force

Spatial inhomogeneities give rise to another non-linear effect which plays a key role in the interaction of intense electromagnetic radiation with plasmas. For consistency we ought to use the full Lorentz equation but to keep the argument simple we revert to non-relativistic dynamics. Let us represent the spatially varying oscillating electric field as

$$\mathbf{E}(\mathbf{r}, t) = \mathbf{E}(\mathbf{r}) \cos \omega t \tag{2.64}$$

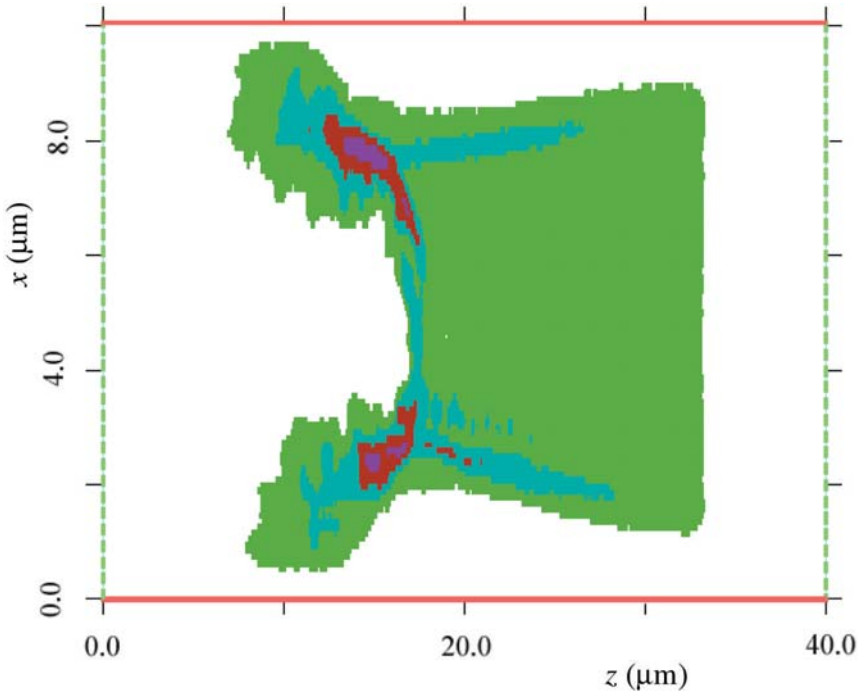

Fig. 2.12. Snapshot of the channel formation in the interaction of laser light of intensity 3×10^{19} W cm^{-2} with a plasma slab. The strong ponderomotive force from the intense laser beam incident from the left forms a channel approximately 4 μm across and 10 μm deep (at 850 fs). White denotes densities below $n_c = 10^{21}$ cm^{-3}, green (1–4)n_c, blue (4–7)n_c, red (7–12)n_c and magenta over $12n_c$ (after Dyson (1998)).

and write $\mathbf{E}(\mathbf{r})$ in terms of an expansion about the initial position of the particle $\mathbf{r}_0$

$$\mathbf{E}(\mathbf{r}) = \mathbf{E}(\mathbf{r}_0) + (\delta\mathbf{r}\cdot\boldsymbol{\nabla})\mathbf{E}|_{\mathbf{r}=\mathbf{r}_0} + \cdots \tag{2.65}$$

To lowest order we use the value $\mathbf{E}(\mathbf{r}_0)$ for the electric field so that the corresponding particle displacement $\delta\mathbf{r}$, is

$$\delta\mathbf{r} = -\frac{e\mathbf{E}}{m\omega^2}\cos\omega t \tag{2.66}$$

To next order we must keep the $\mathbf{v}\times\mathbf{B}$ contribution to the Lorentz equation giving

$$\ddot{\mathbf{r}}_1 = \frac{e}{m}\left[(\delta\mathbf{r}\cdot\boldsymbol{\nabla})\mathbf{E} + \dot{\mathbf{r}}\times\mathbf{B}\right] \tag{2.67}$$